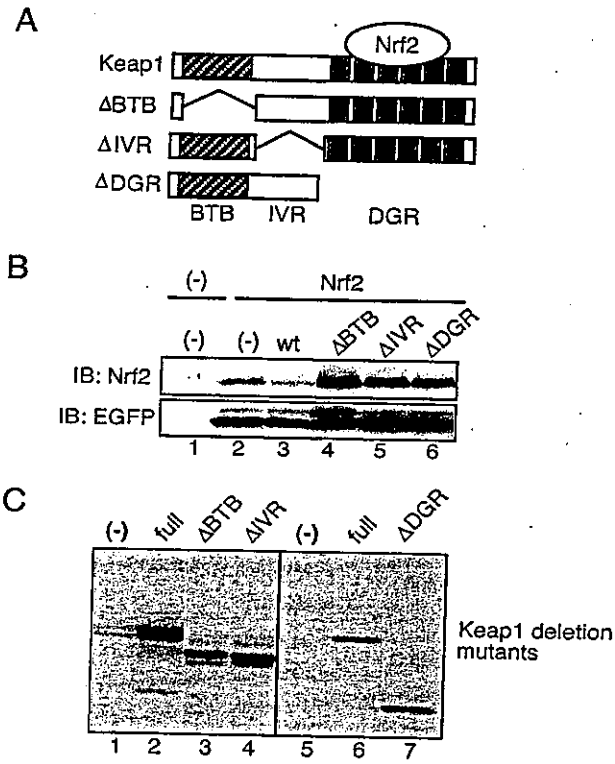

FIG. 3. BTB and IVR domains contribute to degradation of Nrf2 by Keap1. (A) Schematic presentation of Keap1 deletion mutants. Keap1 contains mainly three characteristic domains, the BTB, IVR, and DGR domains. (B) Deletion of the BTB and IVR domains abolished Nrf2 degradation in the in vivo degradation assay (top). The experimental procedure is described in the legend to Fig. 1. The expression of cotransfected EGFP was used as an internal control (bottom). (C) The expression of Keap1 deletion mutants was also monitored by immunoblot analysis with two anti-Keap1 antibodies against the C-terminal and N-terminal ends (lanes 1 to 4 and lanes 5 to 7, respectively). wt, wild type.

We hypothesized that Keap1 might interact with Cul3 through the BTB domain and promote the ubiquitination of Nrf2, thereby resulting in the rapid degradation of Nrf2.

To test this hypothesis, we tested whether Keap1 interacts with Cul3 in vivo through an immunoprecipitation analysis. We immunoprecipitated endogenous Keap1 in 293T cells with an anti-Keap1 antibody and performed an immunoblot analysis with an anti-Cul3 antibody (Fig. 4A). Cul3 was observed in the Keap1 immunocomplex (lane 2), indicating that Keap1 associates with Cul3.

To further clarify the mechanisms of the association of Keap1 with Cul3, we carried out a similar immunoprecipitation analysis but with a DNA transfection system. 293T cells were transfected with Flag-tagged Cul3 and HA-tagged Keap1 expression vectors. Cytoplasmic extracts were prepared from the cells 36 h after transfection and subjected to immunoprecipitation with anti-Flag antibody-conjugated beads. In an immunoblot analysis with anti-HA antibody, HA-tagged Keap1 was clearly visualized in the immunoprecipitates (Fig. 4B), indicating that Keap1 coimmunoprecipitated with Cul3. We also examined the specificity of the association between Keap1 and Cul3 by examining the association of Keap1 with other Cul protein family members by using immunoprecipitation analyses. For this purpose, we expressed Myc-tagged Cul1, Cul2, Cul4A, and Cul5 in 293T cells along with Flag-tagged Keap1. We found that Cul3 specifically interacts with Keap1 whereas the other Cul proteins do not (Fig. 4C). These data thus suggest that Keap1 associates specifically with Cul3 and forms an E3 ligase complex.

The IVR domain of Keap1 associates with the N-terminal region of Cul3. To identify the association interface of Keap1 and Cul3, we performed an immunoprecipitation analysis with 293T cells expressing three Keap1 deletion mutants independently. Since Cul3 was reported to interact with BTB domains, we anticipated that the BTB domain might comprise the interacting interface of Keap1. Surprisingly, however, we could see a positive band to anti-HA antibody in the immunoprecipitates of cell extracts expressing ΔBTB mutant with an anti-Flag antibody (Fig. 5A, lane 3), indicating that deletion of the BTB domain does not abolish the association between Keap1 and Cul3. Similarly, the ΔDGR mutant interacts with Cul3 (lane 5). In contrast, the ΔIVR mutant did not give any positive signals for the anti-HA antibody, indicating that this deletion completely abolishes the interaction with Cul3 (lane 4).

We previously showed that the IVR domain possesses four cysteine residues that bind to the electrophilic agent, dexamethasone 21-mesylate (Dex-mes), (3). Of these four cysteine residues, we further identified Cys273 and Cys288 as playing essential roles in sensing oxidative stress (27). Recently, it was reported that mutation of Cys273 to Ser reduced Keap1-dependent ubiquitination of Nrf2, resulting in the stabilization of Nrf2 (31). Considering these lines of evidence, we next examined the contribution of these cysteine residues to the formation of the Cul3 complex by exploiting cysteine point mutants of Keap1 (Fig. 5B) (27). However, mutation of these cysteine residues within the IVR domain did not significantly affect the association of Keap1 with Cul3, indicating that Cul3 recognizes the interface that is formed by other residues in the IVR domain.

As a reverse strategy, we generated two Cul3 deletion mutants, N280 and ΔN280 (Fig. 5C), and examined their interaction with Keap1. Crystal structure analysis of Cul1 showed that the N-terminal end region of Cul1, which is conserved among the Cul proteins, is the surface of Cul1 that directly associates with the adaptor protein Skp1 (32). Consistent with this observation, Keap1 coimmunoprecipitated with N280 (Fig. 5D, lane 5) but did not recognize the C terminus of Cul3 (lane 7, ΔN280). These results indicate that the association between Keap1 and Cul3 is achieved in an N280 domain-specific manner.

The BTB domain of Bach1 does not bind to Cul3. Although Cul3 was reported to interact with BTB domains, we found that Cul3 recognizes the IVR domain but not the BTB domain of Keap1. To examine whether this nature of Cul3 is specific for Keap1 or can be seen with other proteins, we performed a similar immunoprecipitation analysis with 293T cells expressing Bach1. Bach1 is known to be an Nrf2-related transcription factor and contains a BTB domain (18). We did not detect any positive bands that specifically interacted with an anti-Myc antibody in the immunoprecipitates with an anti-Flag antibody, indicating that Bach1 cannot interact with Cul3 (Fig. 6, lane 4). Since we could clearly reproduce an association between Cul3

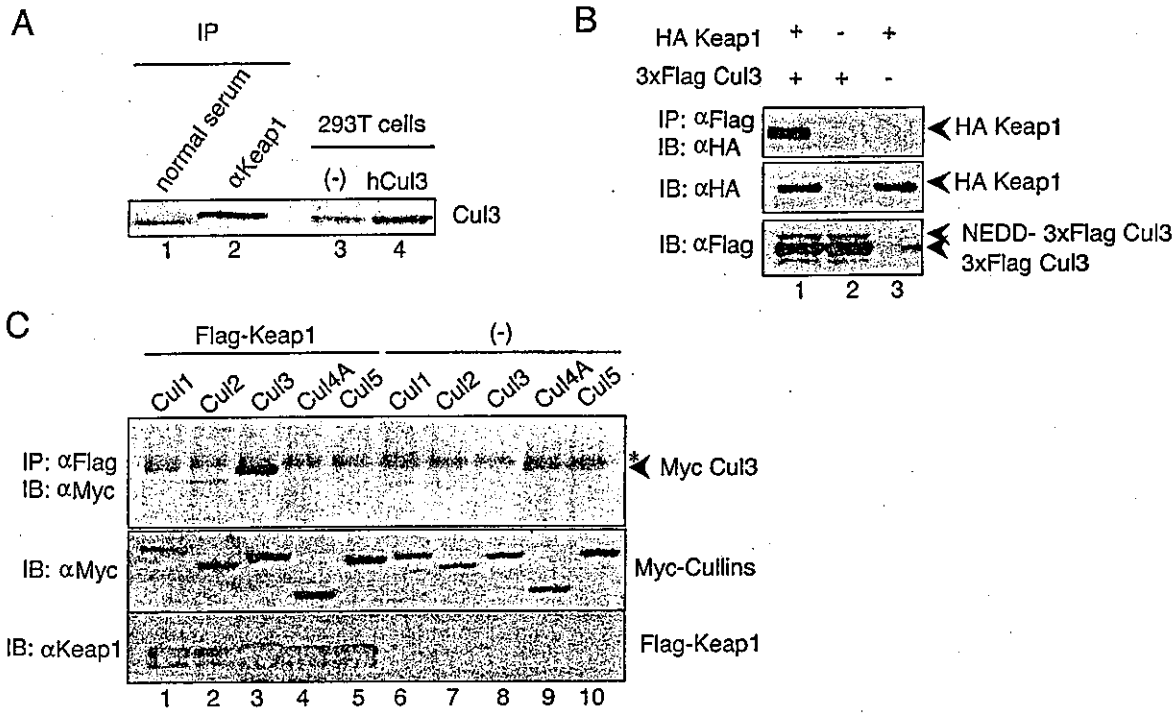

FIG. 4. Keap1 associates specifically with Cul3 in vivo and in vitro. (A) Complex formation of Keap1 and Cul3 in 293T cells. Endogenous Keap1 was precipitated with anti-Keap1 antibody and protein G beads (IP). The immunocomplex was subjected to immunoblot analysis with anti-Cul3 antibody. Whole-cell extracts of 293T cells expressing human Cul3 were used as a control (lanes 3 and 4). (B) Association between Keap1 and Cul3 in a transient-expression system. Whole-cell extracts prepared from 293T cells transfected with expression plasmids of HA-tagged Keap1 (1 μg) and 3xFlag Cul3 (1 μg) were subjected to immunoprecipitation (IP) with anti-Flag (M2) beads and immunoblot analysis with anti-HA antibody (IB). Analyses of cells expressing 3xFlag Cul3 with or without HA-Keap1 (lanes 1 and 2) are shown. Lane 3 is loaded with cell extracts expressing HA-Keap1 alone. (C) Among the Cul family proteins, Cul3 specifically interacts with Keap1. Expression plasmids (1 μg each) of Cul1 (lanes 1 and 6), Cul2 (lanes 2 and 7), Cul3 (lanes 3 and 8), Cul4A (lanes 4 and 9), and Cul5 (lanes 5 and 10) were transfected into 293T cells in the presence (lanes 1 to 5) or absence (lanes 6 to 10) of Flag-fused Keap1. Immunoprecipitation and immunoblot analyses were performed as described above (top). The asterisk indicates a nonspecific band. The expression levels of Cul proteins and Flag-Keap1 were verified by immunoblot analysis with anti-Myc and anti-Keap1 antibodies (middle and bottom, respectively)

and a control BTB protein under the same conditions (data not shown), these data indicate that Cul3 preferentially interacts with certain types of BTB protein as a substrate-specific adaptor.

In vivo ubiquitination of Nrf2 by the Cul3-Keap1 complex. To investigate whether the Keap1-Cul3 complex contributes to the ubiquitination process of Nrf2, we performed an in vivo ubiquitination assay. For this purpose, we transfected into 293T cells the expression plasmids for Nrf2, Keap1, Cul3, and Roc1 (a subunit of the Cul3 complex). We also simultaneously expressed histidine-tagged ubiquitin (26) in the cells. The latter experiment enabled us to purify ubiquitinated Nrf2 by using nickel affinity beads. At 24 h after transfection, the cells were treated with MG132 for 12 h to inhibit the proteasomal degradation of Nrf2. Nrf2 was examined by immunoblot analysis with an anti-Nrf2 antibody.

In the immunoblot analysis, we first examined Nrf2 in the nickel bead precipitates after purification of ubiquitinated Nrf2 from whole-cell extracts (Fig. 7). For the cells expressing wild-type Nrf2, the immunoblot analysis detected multiple bands and showed a smear migration pattern, suggesting that Nrf2 is conjugated with ubiquitin chains in various patterns. Importantly, while the smearing pattern was weak for Nrf2 expressed alone (Fig. 7, upper panel, lane 2), concomitant expression of Keap1 promoted Nrf2 ubiquitination (lane 3). Coexpression of Cul3 and Roc1 enhanced Nrf2 ubiquitination, albeit weakly (lane 5) (see Discussion). In the absence of Keap1, Cul3 plus Roc1 did not provoke ubiquitination of Nrf2 (lane 4). Furthermore, the ΔETGE mutant of Nrf2 did not show this pattern of smearing and ubiquitination (lanes 6 to 9). These results thus demonstrate that the Nrf2 ubiquitination process is strictly dependent on the presence of and interaction with Keap1.

We observed enhancement of Keap1-based Nrf2 ubiquitination by Cul3 and Roc1 more clearly by immunoblot analysis using whole-cell extracts (Fig. 7, lower panel, lanes 2 to 5) than when using nickel affinity column-purified immunoprecipitates. Again, the ΔETGE mutant of Nrf2 that lacks the ability to bind to Keap1 did not effectively promote the ubiquitination of Nrf2 (lanes 6 to 9). Taken together, these data demonstrate that the Keap1-Cul3 complex ubiquitinates Nrf2 and regulates the turnover of Nrf2.

DISCUSSION

In this study, we aimed to clarify the molecular mechanisms governing rapid Nrf2 turnover and the contribution of Keap1 to this degradation pathway. We revealed that the rapid degradation of Nrf2 requires direct association with Keap1. We

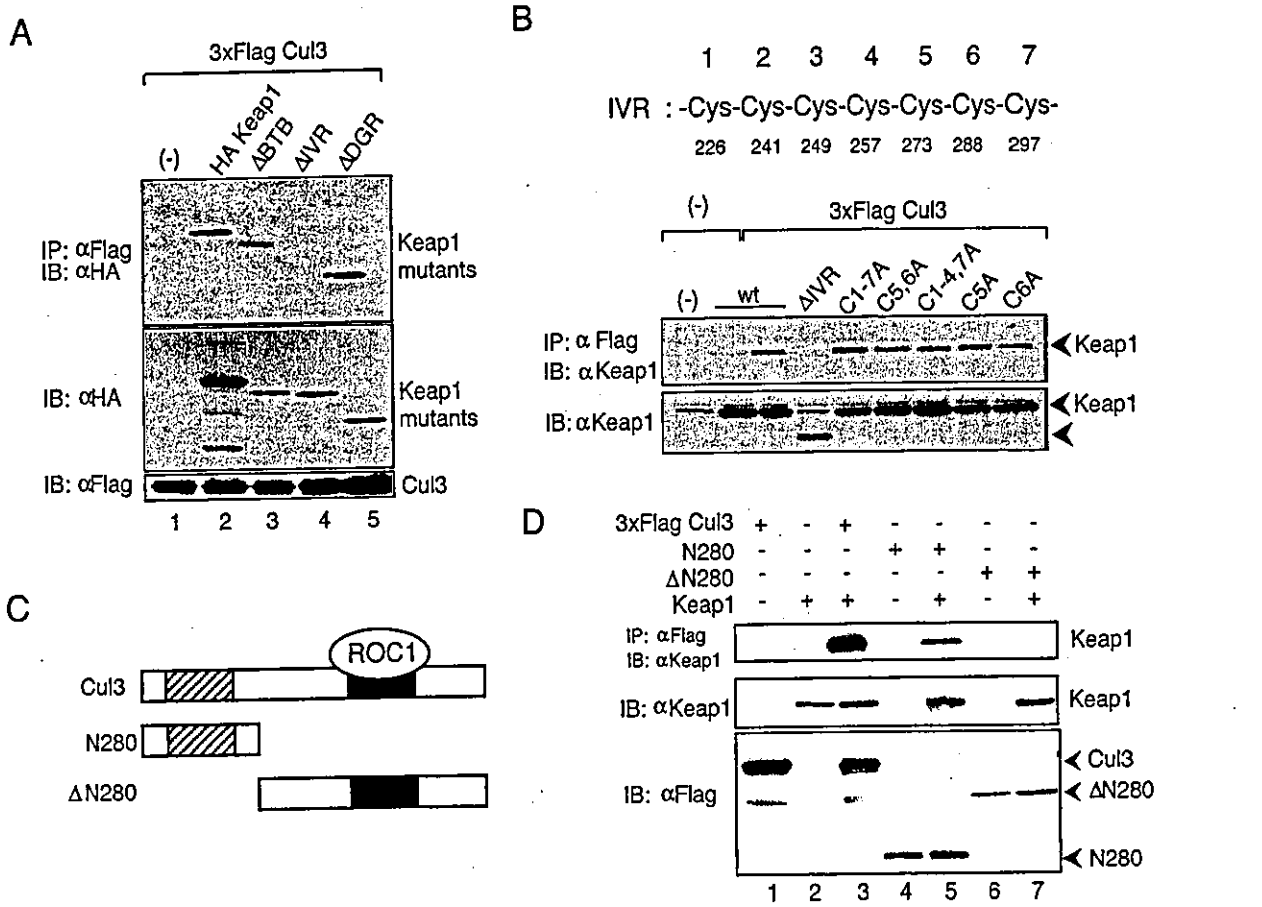

FIG. 5. The IVR domain of Keap1 associates with the N-terminal end of Cul3. (A) Whole-cell extracts prepared from 293T cells transfected with various expression plasmids of HA-tagged Keap1 deletion mutants (1 μg) and 3xFlag tagged Cul3 (1 μg) were subjected to an immunoprecipitation (IP) assay with anti-Flag antibody beads and immunoblot (IB) analysis with anti-HA antibody (top). The expression levels of Keap1 deletion mutants and 3xFlag Cul3 were verified by immunoblot analysis with anti-HA and anti-Flag antibodies (middle and bottom, respectively). Analyses of cell lysates coexpressing 3xFlag Cul3 and HA-Keap1 (lane 2), ΔBTB (lane 3), ΔIVR (lane 4), or ΔDGR (lane 5) are shown. Lane 1 is loaded with cell extract expressing only 3xFlag Cul3. (B) Cysteine residues in the IVR domain are not crucial for the association between Keap1 and Cul3. The IVR contains seven cysteine residues (from Cys226 to Cys297), renumbered arbitrarily from 1 to 7. The association between Cul3 and Keap1 Cys point mutants (27) was examined by immunoprecipitation (upper panel) as described above. The expression levels of Cys mutants were verified by immunoblot analysis with anti-Keap1 antibody (lower panel). (C) Schematic presentation of Cul3 deletion mutants. (D) The N-terminal sequence of Cul3 is crucial for its association with Keap1. Whole-cell extracts of 293T cells transfected with expression plasmids of Cul3 deletion mutants (1 μg) and Keap1 (1 μg) were prepared and subjected to immunoprecipitation with anti-Flag (M2) beads and immunoblotting with anti-Keap1 antibody. Analyses of cell lysates expressing 3xFlag Cul3 (lanes 1 and 3), N280 (lanes 4 and 5), or ΔN280 (lanes 6 and 7) in the presence (lanes 2, 3, 5, and 7) or absence (lanes 1, 4, and 6) of Keap1 are shown (top). The expression levels of Keap1 and Cul3 deletion mutants were verified by immunoblot analysis with anti-Keap1 and anti-Flag antibodies (middle and bottom, respectively)

also found that the IVR domain of Keap1 specifically interacts with Cul3, a component of the E3 ligase complex. These results provide the first convincing evidence for proteasomal degradation of Nrf2 and the function of Keap1 as an adaptor for Cul3-based E3 ligase (Fig. 8). The critical stress-responsive transcription factors IκB, Hif-1α, and Nrf2 have now been shown to share the ubiquitin-proteasome system in their rapid turnover and to use specific Cul-type E3 ligases, with IκB, Hif-1α, and Nrf2 using Cul1, Cul2, and Cul3, respectively. To our knowledge, Nrf2 and Keap1 are the first mammalian substrate and adaptor reported for the Cul3-based E3 ligase system.

While Cul3 in *Caenorhabditis elegans* was reported to ubiquitinate the substrate MEI-1/katanin through MEL26 as an adaptor (20, 21), the molecular mechanisms of Cul3 activity remain to be elucidated. A subset of proteins harboring the BTB domain were recently reported to serve as an adaptor in the Cul3-based E3 ligase system (4, 5, 21, 30). Our present data indicate that the BTB domain of Keap1 is necessary for Keap1 to function as an accelerator of Nrf2 degradation. However, one unexpected finding in this study is that deletion of the BTB domain does not significantly affect the association of Keap1 with Cul3. Rather, Keap1 effectively associates with Cul3 through the IVR domain. The BTB domain of Bach1 does not bind to Cul3 either (Fig. 6), demonstrating that not all BTB domains interact with Cul3.

The molecular mechanism by which the IVR domain interacts with Cul3 is unclear at present. Zhang and Hannink recently reported that mutation of the reactive cysteines Cys273 and Cys288 in the IVR domain repressed Nrf2 degradation

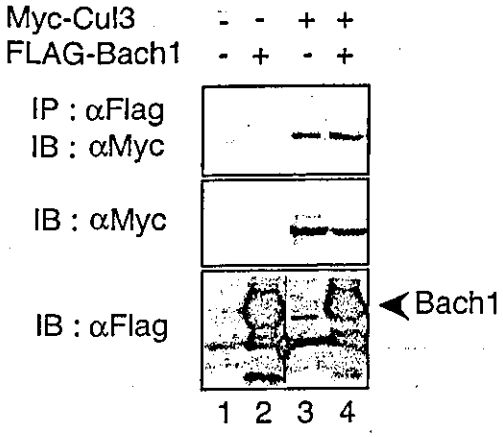

FIG. 6. The BTB domain of Bach1 does not bind Cul3. Whole-cell extracts prepared from 293T cells transfected with expression plasmids (3 μg) in the combinations indicated were subjected to immunoprecipitation (IP) with anti-Flag antibody-conjugated beads followed by immunoblot (IB) analysis with an anti-Myc antibody (top). The expression level of each protein was monitored by immunoblot analysis with anti-Myc (middle) and anti-Flag (bottom) antibodies, respectively.

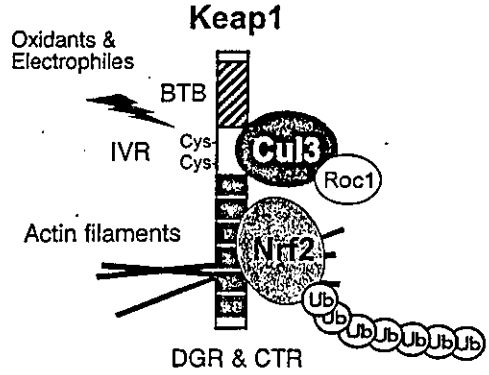

FIG. 8. Schematic model of the Keap1-Cul3 complex function as an E3 ligase. The cytoplasmic factor Keap1, bound on actin filaments, acts as a sensor for oxidative and electrophilic stress through two cysteine residues in the IVR domain. In the absence of stimuli, Keap1 sequesters the transcription factor Nrf2, a major regulator of the oxidative stress response, in the cytoplasm. In addition, Keap1 functions as an adaptor of the Cul3-based E3 ligase. This E3 ligase conjugates ubiquitin to Nrf2 and promotes rapid degradation of Nrf2 by proteasome in order to inhibit the expression of oxidative stress response genes under normal conditions.

due to an impaired ubiquitin pathway (31). Based on their observation, they proposed the hypothesis that these two cysteines in the IVR domain are crucial for the complex formation between Keap1 and an unknown E3 ligase. Although our present data indicate that Cul3 recognizes the IVR domain, our data clearly show that Cul3 binds to Keap1 despite mutations in the two reactive cysteines, indicating that Cul3 recognizes an alternative motif in the IVR domain. Furthermore, alanine substitutions of both Cys273 and Cys288 did not affect the ubiquitination of Nrf2 (data not shown). Thus, the present results disagree with their report, so this point remains to be clarified.

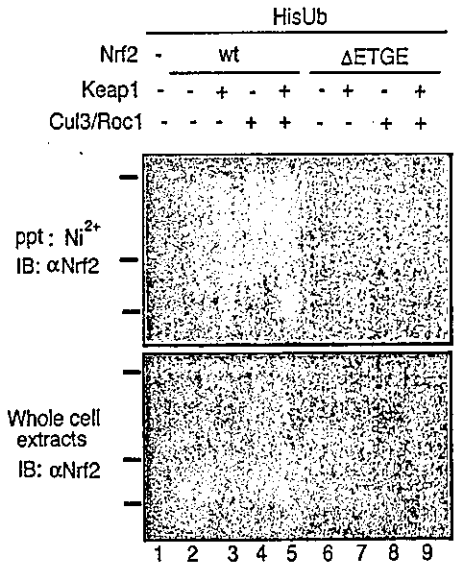

FIG. 7. Ubiquitination of Nrf2 by Keap1 and Cul3 in vivo. Nrf2 (1 μg) was expressed in 293T cells, along with several combinations of Keap1 (0.5 μg) and Cul3 (1.5 μg)-Roc1 (1 μg), as indicated in the figure, in the presence of His-tagged ubiquitin (HisUb; 1 μg). As a control, the ΔETGE mutant was also transfected. Whole-cell extracts were prepared and subjected to affinity purification with Ni^{2+} resin. Precipitates (ppt) were eluted by boiling in sodium dodecyl sulfate sample buffer and subjected to immunoblot (IB) analysis (upper panel) with anti-Nrf2 antibody. The expression level of Nrf2 in the whole-cell extracts was also verified by immunoblot analysis with anti-Nrf2 antibody (lower panel).

We envisage that two lines of evidence may be pertinent in this regard. First, the electrophilic reagent Dex-mes binds to the two reactive cysteines in the IVR domain (3) and liberates Nrf2 from Keap1. Second, Keap1 containing alanine substitutions of both Cys273 and Cys288 did not effectively repress the transactivation activity of Nrf2 in a cell culture system (27). Based on these observations, we propose that the two reactive cysteine residues in the IVR regulate the association of Keap1 with Nrf2.

Our results in Fig. 3 suggest that the BTB domain of Keap1 contributes to the turnover of the Nrf2 protein. Consistent with these data Zipper and Mulcahy (33) showed that the BTB domain of Keap1 is crucial for its dimerization and negative regulation of Nrf2. Furthermore, Zhang and Hannink (31) have recently reported that a C151S Keap1 mutation in the BTB domain significantly reduced Nrf2 activation in response to oxidants (31). Thus, while our analysis indicates that Cys151 is not a direct target of Dex-mes conjugation (3), it seems likely that this residue contributes to the function of Keap1. Further work to clarify the role of BTB in the Keap1/Nrf2 pathway is required.

Stresses on the endoplasmic reticulum were recently reported to activate the Nrf2-Keap1 system through direct phosphorylation of Nrf2 by pancreatic endoplasmic reticulum eukaryotic initiation factor 2α kinase (2). This observation suggests that the Nrf2-Keap1 system can be activated by signals other than oxidative stress. The ubiquitin-like protein NEDD8 regulates the E3 ligase activity of Cul3 by covalent modification, which is essential for the association of Cul3 with E2

enzyme (8, 20). The Cul3 complex contains a COP9 signalosome that functions as a deneddylation enzyme (1, 29). Hence, one emerging hypothesis is that down-regulation of Cul3 activity by deneddylation may enable Nrf2 stabilization, by which signals can induce the expression of cytoprotective target genes. Supporting this notion, the addition of a proteasome inhibitor was reported to induce the expression of the GCL gene, which encodes the catalytic subunit of γ-glutamylcysteine synthetase (22). Under our present experimental conditions, however, we could not detect the promotion of NEDD8 modification of Cul3 by oxidative stress (data not shown). Nonetheless, we feel that it is still of interest to explore this hypothesis.

The Neh2 domain of Nrf2 is ubiquitinated in a Keap1-dependent manner and possesses seven lysine residues, some of which might be conjugated with a polyubiquitin chain (Y. Kato, K. Itoh, and M. Yamamoto, submitted for publication). In addition, deletion of the C-terminal Neh1, Neh3, and Neh6 domains of Nrf2 renders the protein more stable than full-length Nrf2 (Fig. 1 and 2, compare 7.5 and 25 min, respectively), suggesting that Nrf2 contains an alternative degradation signal in this C-terminal portion. We previously showed two modes of Nrf2 degradation, namely, Keap1-dependent degradation in the cytoplasm and Keap1-independent degradation in the nucleus (9). The turnover of Nrf2 by the latter pathway is slower than that by the former. We surmise that Nrf2 degradation in the nucleus also uses the proteasome pathway but must be Cul3 independent. Therefore, the next important task would be to identify an E3 ligase complex that is essential for the nuclear degradation of Nrf2.

We exploited Cul3 double-stranded RNA (dsRNA) in a preliminary examination to assess whether endogenous Cul3 regulates the degradation of Nrf2 in collaboration with Keap1. Cul3 dsRNA was transfected into HeLa cells, and cyclin E was first analyzed as a control, since Cul3 was reported to determine the stability of cyclin E in the ubiquitin-proteasome system (24). However, although transfection of Cul3 dsRNA significantly affected the expression of Cul3 mRNA, only a marginal accumulation of cyclin E was found (data not shown). Similarly, down-regulation of Cul3 did not affect the stability of endogenous Nrf2 (data not shown). One plausible explanation for this observation is that because the dsRNA did not completely abrogate the Cul3 protein, the residual small amount of Cul3 might have been enough for rapid degradation of Nrf2 to take place. Supporting this hypothesis, we found that expression of Keap1 alone significantly enhanced the ubiquitination of Nrf2 in an in vivo ubiquitin assay whereas further expression of Cul3 and Roc1 enhanced ubiquitination only marginally (Fig. 7). These results suggest that Cul3 and Roc1 are abundant within living cells. An alternative explanation is that Keap1-independent degradation, as described above, might compensate for the loss of Cul3 function.

The function of Keap1 as an E3 ligase adaptor has similarity to the function of pVHL. It has been well documented that multiple human diseases are provoked by mutations in pVHL. These mutations usually affect the function of pVHL as an adaptor and cause aberrant stabilization of Hif-1α (11). Thus, cellular homeostasis requires not only inducible activation of transcription factors in response to stress stimuli but also continuous inactivation of the transcription factors through their rapid degradation or subcellular compartmentalization during unstressed conditions. Interestingly, a subset of Cul proteins requires WD40 repeat proteins as an adaptor to target substrates. This WD40 repeat domain is known to form a β-barrel structure (28). The DGR domain of Keap1 also forms a β-barrel structure. These observations further support our contention that Cul-based E3 ligases have common properties in both function and structure.

ACKNOWLEDGMENTS

We are grateful to Tomohiko Ohta, Dirk Bohmann, and Tae Yamamoto for their generous donation of plasmids. We also thank Ken Itoh, Hozumi Motohashi, Makoto Kobayashi, Yasutake Kato, and Tania O'Connor for discussion and advice.

This work was supported in part by grants-in-aid from JST-ERATO (M.Y.), Ministry of Education, Sports, Science and Technology (A.K. and M.Y.), Ministry of Health, Labor and Welfare (M.Y.), Atherosclerosis Foundation (M.Y.), and Naito Foundation (M.Y.).

REFERENCES

1. **Cope, G. A., and R. J. Deshaies.** 2003. COP9 signalosome: a multifunctional regulator of SCF and other cullin-based ubiquitin ligases. Cell 114:663–671.
2. **Cullinan, S. B., D. Zhang, M. Hannink, E. Arvisais, R. J. Kaufman, and J. A. Diehl.** 2003. Nrf2 is a direct PERK substrate and effector of PERK-dependent cell survival. Mol. Cell. Biol. 23:7198–7209.
3. **Dinkova-Kostova, A. T., W. D. Holtzclaw, R. N. Cole, K. Itoh, N. Wakabayashi, Y. Katoh, M. Yamamoto, and P. Talalay.** 2002. Direct evidence that sulfhydryl groups of Keap1 are the sensors regulating induction of phase 2 enzymes that protect against carcinogens and oxidants. Proc. Natl. Acad. Sci. USA 99:11908–11913.
4. **Furukawa, M., Y. J. He, C. Borchers, and Y. Xiong.** 2003. Targeting of protein ubiquitination by BTB-Cullin 3-Roc1 ubiquitin ligases. Nat. Cell Biol. 5:1001–1007.
5. **Geyer, R., S. Wee, S. Anderson, J. Yates, and D. A. Wolf.** 2003. BTB/POZ domain proteins are putative substrate adaptors for cullin 3 ubiquitin ligases. Mol. Cell 12:783–790.
6. **Hayes, J. D., S. A. Chanas, C. J. Henderson, M. McMahon, C. Sun, G. J. Moffat, C. R. Wolf, and M. Yamamoto.** 2000. The Nrf2 transcription factor contributes both to the basal expression of glutathione S-transferases in mouse liver and to their induction by the chemopreventive synthetic antioxidants, butylated hydroxyanisole and ethoxyquin. Biochem. Soc. Trans. 28:33–41.
7. **Hershko, A., and A. Ciechanover.** 1998. The ubiquitin system. Annu. Rev. Biochem. 67:425–479.
8. **Hori, T., F. Osaka, T. Chiba, C. Miyamoto, K. Okabayashi, N. Shimbara, S. Kato, and K. Tanaka.** 1999. Covalent modification of all members of human cullin family proteins by NEDD8. Oncogene 18:6829–6834.
9. **Itoh, K., N. Wakabayashi, Y. Katoh, T. Ishii, T. O'Connor, and M. Yamamoto.** 2003. Keap1 regulates both cytoplasmic-nuclear shuttling and degradation of Nrf2 in response to electrophiles. Genes Cells 8:379–391.
10. **Itoh, K., T. Ishii, N. Wakabayashi, and M. Yamamoto.** 1999. Regulatory mechanisms of cellular response to oxidative stress. Free Radic. Res. 31: 319–324.
11. **Kaelin, W. G., Jr.** 2002. Molecular basis of the VHL hereditary cancer syndrome. Nat. Rev. Cancer 2:673–682.
12. **Kang, M.-I., A. Kobayashi, N. Wakabayashi, S. G. Kim, and M. Yamamoto.** 2004. Scaffolding of Keap1 to the actin cytoskeleton controls the function of Nrf2 as key regulator of cytoprotective phase 2 genes. Proc. Natl. Acad. Sci. USA 101:2046–2051.
13. **Kobayashi, M., K. Itoh, T. Suzuki, H. Osanai, K. Nishikawa, Y. Katoh, Y. Takagi, and M. Yamamoto.** 2002. Identification of the interactive interface and phylogenic conservation of the Nrf2-Keap1 system. Genes Cells 7:807–820.
14. **Levonen, A. L., A. Landar, A. Ramachandran, E. K. Ceaser, D. A. Dickinson, G. Zanoni, J. D. Morrow, and V. M. Darley-Usmar.** 2004. Cellular mechanisms of redox cell signaling: role of cysteine modification in controlling antioxidant defenses in response to electrophilic lipid oxidation products. Biochem. J. 378:373–382.
15. **McMahon, M., K. Itoh, M. Yamamoto, and J. D. Hayes.** 2003. Keap1-dependent proteasomal degradation of transcription factor Nrf2 contributes to the negative regulation of antioxidant response element-driven gene expression. J. Biol. Chem. 278:21592–21600.
16. **Nguyen, T., P. J. Sherratt, and C. B. Pickett.** 2003. Regulatory mechanisms controlling gene expression mediated by the antioxidant response element. Annu. Rev. Pharmacol. Toxicol. 43:233–260.
17. **Nguyen, T., P. J. Sherratt, H. C. Huang, C. S. Yang, and C. B. Pickett.** 2003.

Increased protein stability as a mechanism that enhances Nrf2-mediated transcriptional activation of the antioxidant response element. Degradation of Nrf2 by the 26 S proteasome. J. Biol. Chem. 278:4536–4541.
18. Oyake, T., K. Itoh, H. Motohashi, N. Hayashi, H. Hoshino, M. Nishizawa, M. Yamamoto, and K. Igarashi. 1996. Bach proteins belong to a novel family of BTB-basic leucine zipper transcription factors that interact with MafK and regulate transcription through the NF-E2 site. Mol. Cell. Biol. 16:6083–6095.
19. Pickart, C. M. 2001. Ubiquitin enters the new millennium. Mol. Cell 8:499–504.
20. Pintard, L., T. Kurz, S. Glaser, J. H. Willis, M. Peter, and B. Bowerman. 2003. Neddylation and deneddylation of CUL-3 is required to target MEI-1/katanin for degradation at the meiosis-to-mitosis transition in *C. elegans*. Curr. Biol. 13:911–921.
21. Pintard, L., J. H. Willis, A. Willems, J. L. Johnson, M. Srayko, T. Kurz, S. Glaser, P. E. Mains, M. Tyers, B. Bowerman, and M. Peter. 2003. The BTB protein MEL-26 is a substrate-specific adaptor of the CUL-3 ubiquitin-ligase. Nature 425:311–316.
22. Sekhar, K. R., S. R. Soltaninassab, M. J. Borrelli, Z. Q. Xu, M. J. Meredith, F. E. Domann, and M. L. Freeman. 2000. Inhibition of the 26S proteasome induces expression of GLCLC, the catalytic subunit for gamma-glutamylcysteine synthetase. Biochem. Biophys. Res. Commun. 270:311–317.
23. Semenza, G. L. 2001. HIF-1 and mechanisms of hypoxia sensing. Curr. Opin. Cell Biol. 13:167–171.
24. Singer, J. D., M. Gurian-West, B. Clurman, and J. M. Roberts. 1999. Cullin-3 targets cyclin E for ubiquitination and controls S phase in mammalian cells. Genes Dev. 13:2375–2387.
25. Stewart, D., E. Killeen, R. Naquin, S. Alam, and J. Alam. 2003. Degradation of transcription factor Nrf2 via the ubiquitin-proteasome pathway and stabilization by cadmium. J. Biol. Chem. 278:2396–2402.
26. Treier, M., L. M. Staszewski, and D. Bohmann. 1994. Ubiquitin-dependent c-Jun degradation in vivo is mediated by the delta domain. Cell 78:787–798.
27. Wakabayashi, N., A. T. Dinkova-Kostova, W. D. Holtzclaw, M-I. Kang, A. Kobayashi, M. Yamamoto, T. W. Kensler, and P. Talalay. 2004. Protection against electrophile and oxidant stress by induction of the phase 2 response: Fate of cysteines of the Keap1 sensor modified by inducers. Proc. Natl. Acad. Sci. USA 101:2040–2045.
28. Wall, M. A., D. E. Coleman, E. Lee, J. A. Iniguez-Lluhi, B. A. Posner, A. G. Gilman, and S. R. Sprang. 1995. The structure of the G protein heterotrimer Gi alpha 1 beta 1 gamma 2. Cell 83:1047–1058.
29. Wolf, D. A., C. Zhou, and S. Wee. 2003. The COP9 signalosome: an assembly and maintenance platform for cullin ubiquitin ligases? Nat. Cell Biol. 5:1029–1033.
30. Xu, L., Y. Wei, J. Reboul, P. Vaglio, T. H. Shin, M. Vidal, S. J. Elledge, and J. W. Harper. 2003. BTB proteins are substrate-specific adaptors in an SCF-like modular ubiquitin ligase containing CUL-3. Nature 425:316–321.
31. Zhang, D. D., and M. Hannink. 2003. Distinct cysteine residues in Keap1 are required for Keap1-dependent ubiquitination of Nrf2 and for stabilization of Nrf2 by chemopreventive agents and oxidative stress. Mol. Cell. Biol. 23: 8137–8151.
32. Zheng, N., B. A. Schulman, L. Song, J. J. Miller, P. D. Jeffrey, P. Wang, C. Chu, D. M. Koepp, S. J. Elledge, M. Pagano, R. C. Conaway, J. W. Conaway, J. W. Harper, and N. P. Pavletich. 2002. Structure of the Cul1-Rbx1-Skp1-F boxSkp2 SCF ubiquitin ligase complex. Nature 416:703–709.
33. Zipper, L. M., and R. T. Mulcahy. 2002. The Keap1 BTB/POZ dimerization function is required to sequester Nrf2 in cytoplasm. J. Biol. Chem. 277: 36544–36552.

Available online at www.sciencedirect.com
SCIENCE DIRECT®
Biochemical and Biophysical Research Communications 321 (2004) 72–79
BBRC
www.elsevier.com/locate/ybbrc

Identification of polymorphisms in the promoter region of the human *NRF2* gene

Tae Yamamoto [a,1], Keigyou Yoh [a,1], Akira Kobayashi [a], Yukio Ishii [a], Shigeo Kure [d], Akio Koyama [a], Tohru Sakamoto [a], Kiyohisa Sekizawa [a], Hozumi Motohashi [a,*], Masayuki Yamamoto [a,b,c,*]

[a] *Graduate School of Comprehensive Human Sciences, Majors of Medical Sciences, University of Tsukuba, 1-1-1 Tennoudai, Tsukuba 305-8577, Japan*
[b] *Center for Tsukuba Advanced Research Alliance, University of Tsukuba, 1-1-1 Tennoudai, Tsukuba 305-8577, Japan*
[c] *Environmental Response Project, Exploratory Research for Advanced Technology-Japan Science and Technology Corporation, University of Tsukuba, 1-1-1 Tennoudai, Tsukuba 305-8577, Japan*
[d] *Department of Medical Genetics, Tohoku University School of Medicine, Sendai 980-8574, Japan*

Received 15 June 2004
Available online 10 July 2004

Abstract

Transcription factor Nrf2 regulates the basal and inducible expression of detoxifying and antioxidant genes. Recent studies using *nrf2*-null mice suggest that Nrf2 dysfunction might be involved in the pathogenesis of human diseases. To gain insight into the relationship between impairment in the *NRF2* gene and human diseases, we attempted to identify polymorphisms in the human *NRF2* gene. We determined the structure of the *NRF2* gene and found three single nucleotide polymorphisms and one triplet repeat polymorphism in its regulatory region. These results provide a molecular basis for the genetic analysis of the *NRF2* gene. The frequency of each polymorphism was examined in two groups of patients with systemic lupus erythematosus and chronic obstructive pulmonary disease. This study did not reveal a close connection between the risk of these diseases and the polymorphisms. However, available lines of evidence suggest the importance of examining the link between *NRF2* polymorphisms and other oxidative stress-related diseases.

Keywords: Human *NRF2* gene; Transcription; Initiator site; Promoter; Polymorphism; SNP; Japanese; 5′-RACE; RNase protection; Systemic lupus erythematosus; Chronic obstructive pulmonary diseases

Nrf2 belongs to the CNC family of transcription factors harboring a characteristic basic-leucine zipper (b-Zip) motif and is essential for the basal and inducible expression of a battery of detoxifying and antioxidative enzyme/protein genes [1–3]. Nrf2-deficient mice are susceptible to xenobiotic and oxidative stress owing to an impaired expression of their cytoprotective enzymes. Consequently, Nrf2-deficient mice display various pathological phenotypes, some of which are similar or related to human disorders [4–7]. For instance, systemic exposure to butylated hydroxytoluene and acetaminophen leads to acute pulmonary injury [4] and acute hepatotoxicity [5], respectively. Inhalation of diesel exhaust results in the accumulation of high levels of DNA adducts [6]. Mechanisms underlying cancer chemoprevention are also defective in Nrf2-deficient mice [7,8], with oltipraz and sulforaphane failing to exert their protective effects against xenobiotic-induced carcinogenesis, thus indicating the critical roles that Nrf2 plays in cancer chemoprevention.

Recent studies also unveiled that Nrf2 is an important regulator of oxidative stress-inducible genes, such

* Corresponding authors. Fax: +81-29-853-7318.
E-mail address: masi@tara.tsukuba.ac.jp (M. Yamamoto).
[1] These two authors equally contributed to this work.

0006-291X/$ - see front matter © 2004 Elsevier Inc. All rights reserved.
doi:10.1016/j.bbrc.2004.06.112

as heme oxygenase-1 and peroxiredoxin 1 [9]. Susceptibility to hyperoxia turned out to be tightly linked to the *nrf2* locus [10]. A single nucleotide polymorphism was detected in the promoter region of the *nrf2* gene belonging to C57BL/6J mice, a strain sensitive to hyperoxic stress. Supporting this contention, *nrf2*-null mutant mice were found to be highly susceptible to hyperoxic lung injury [11]. Electron paramagnetic resonance (EPR) and spin probe kinetic analysis showed that the impaired defense mechanism against oxidative stress in the liver and kidney of *nrf2*-null mutant mice substantially decreases the ability to eliminate reactive oxygen species (ROS) [12]. It has been assumed that ROS play a prominent role in the pathogenesis of various human diseases including nephritis. The impaired elimination of ROS is exacerbated in aged female Nrf2-deficient animals [12]. In fact, elderly female *nrf2* -deficient mice often develop lupus-like autoimmune nephritis [13].

Available evidence indicates that the activation of Nrf2 is an important cue for the inducible expression of cytoprotective genes. Exposure to electrophilic reagents dissociates Nrf2 from its cytoplasmic repressor Keap1, resulting in stabilized Nrf2 which is free to translocate from the cytoplasm to the nucleus [14–18]. In some cell lineages, transcription of the *nrf2* gene is also facilitated in response to stress stimuli, implying the presence of a positive feedback system to attain a high level of Nrf2 expression [19].

These analyses using Nrf2-deficient animals led us to hypothesize that the dysregulation of Nrf2 activity may explain, at least in part, the pathogenesis of certain human diseases. To address this issue further, we attempted to search the human *NRF2* gene locus for polymorphisms. To this end, we determined the structure of the *NRF2* gene and identified its transcription initiation site using extension and protection methods. We then determined the nucleotide sequences of the gene from healthy volunteers, and found three SNPs and one triplet repeat polymorphism in the regulatory region. We could not find any polymorphisms in the coding exons. Thus, this study provides a solid molecular basis for the genetic analyses of the human *NRF2* gene. In our preliminary analysis, the frequencies of the promoter polymorphisms were examined in healthy and disease-prone Japanese populations, especially those with systemic lupus erythematosus (SLE) and chronic obstructive pulmonary disease (COPD). While we were unable to find a close relationship between the identified polymorphisms and SLE or COPD, we feel it is highly likely that a significant association between certain diseases and the polymorphisms identified in this study may become apparent if a more adequate population is selected.

Materials and methods

Oligonucleotides and human NRF2 plasmids. The oligonucleotides used for PCR and 5′-rapid amplification of the cDNA ends (RACE) are shown in Tables 1 and 2. The genomic PCR oligonucleotides were designed for the detection of polymorphisms so that the dye–primer sequence reaction could be followed directly; an 18 bp oligonucleotide (5′-tgtaaaacgacggccagt-3′) was attached to the 5′-ends of forward

Table 1
Sequence of oligonucleotides used for 5′-RACE, RPA, and promoter sequencing

Name	Sequence
5′-RACE primers	
E2/89-68	5′-TACTCTTTCCGTCGCTGACTGAA-3′
E2/64-35	5′-CAAATACTTCTCGACTTACTCCAAGATCTA-3′
Primers for making RPA probes	
Probe/A-F	5′-ccgcggatccCGGGCGGTAAAGTGAGATAA-3′
Probe/B-F	5′-ccgcggatccGGGATTTTCGGAAGCTCAG-3′
Exon 1-R1	5′-GAGCTGTGGACCGTGTGTT-3′
Exon 1-F1	5′-ATCATGATGGACTTGGAGCTG-3′
Probe/E2-R	5′-gccggaattCTGGTTTCTGACTGGATGTGC-3′
Exon 1-R2	5′-GCAGCTCCAAGTCCATCAT-3′
Primers for genotyping polymorphism	
hNrf2/P2-F	5′-tgtaaaacgacggccagtGCGTGGTGGCTGCGCTTT-3′
hNrf2/P2-R	5′-caggaaacagctatgaccGCCCGCGAGATAAAGAGTTG-3′
hNrf2/E1-F	5′-tgtaaaacgacggccagtCGTGTAGCCGATTACCGAGTGCC-3′
hNrf2/E1-R	5′-caggaaacagctatgaccCTCTGGCCAGACGTGGGGGAAG-3′
hN/E1g-F	5′-Cy5-TAGCCGATTACCGAGTGCCG-3′
hN/E1g-R	5′-GGCAGCTCCAAGTCCATCATG-3′

Upper-case letters represent the sequences derived from the human *NRF2* gene locus, while lower-case letters represent synthetic sequences. *Bam*HI and *Eco*RI restriction sites are underlined. Synthetic sequences attached to the 5′-ends of primers for genotyping were hybridized by the dye-primers used in an ABI PRISM BigDye Primer Cycle Sequencing Ready Reaction Kit for direct sequencing analysis. The 5′-end of hNE1g-F was modified with Cy5 for gene scan analysis for genotyping the triplet polymorphism.

Table 2
Sequence of oligonucleotides used for sequencing the coding region of the human *NRF2* gene

Name	Sequence
hNrf2/E2-F	5′-tgtaaaacgacggccagtACCATCAACAGTGGCATAATGTG-3′
hNrf2/E2-R	5′-caggaaacagctatgaccGCAAAGCTGGAACTCAAATCCAG-3′
hNrf2/E3-F	5′-tgtaaaacgacggccagtATTATTGAATATTTAGCTTGGC-3′
hNrf2/E3-R	5′-caggaaacagctatgaccGGAGATTCATTGACGGGACTTAC-3′
hNrf2/E4-F	5′-tgtaaaacgacggccagtTGTAGTGGTGCCTTAGAGCTTAC-3′
hNrf2/E4-R	5′-caggaaacagctatgaccAATAGCACCCTCCAATCCTTCC-3′
hNrf2/E5a-F	5′-tgtaaaacgacggccagtCTGAAGATAATGTGGGTAGGGAG-3′
hNrf2/E5a-R	5′-caggaaacagctatgaccCATTCTGTTTGACACTTCCAGGG-3′
hNrf2/E5b-F	5′-tgtaaaacgacggccagtTGATTCTGAAGTGGAAGAGCTAG-3′
hNrf2/E5b-R	5′-caggaaacagctatgaccCTAAATCTTGCTCTAGTTCTAC-3′
hNrf2/E5c-F	5′-tgtaaaacgacggccagtGTAAGAATAAAGTGGCTGCTCAG-3′
hNrf2/E5c-R	5′-caggaaacagctatgaccTCAACATACTGACACTCCAATGC-3′

Upper-case letters represent the sequences derived from the human *NRF2* gene locus, while lower-case letters represent synthetic sequences.

primers and an 18 bp oligonucleotide (5′-caggaaacagctatgacc-3′) was attached to the 5′-ends of reverse primers. One of the primers for gene scan (hN/E1g-F) was modified at the 5′-end with Cy5. The plasmid harboring the human NRF2 cDNA (pcDNAI/hNRF2) was a kind gift from Dr. Etsuro Ito, and the P1 phage containing the human *NRF2* gene was from Genome Systems.

Cell culture and RNA isolation. To isolate human total RNA, Jurkat, HeLa, and Hep3B cells were maintained in DMEM (Sigma) supplemented with 10% fetal bovine serum, 50 U/ml penicillin, and 50 μg/ml streptomycin. These cells were incubated at 37 °C in 5% CO_2 until sub-confluency. The cells were harvested in Isogen (Nippon Gene) to isolate total RNAs.

5′-RACE analysis. Poly(A)$^+$ RNA was purified from 250 μg total Jurkat cell RNA using Oligotex-MAG mRNA purification kit (TaKaRa), and 5′-RACE analysis was carried out with SMART RACE cDNA Amplification Kit (Clontech Laboratories). Two reverse primers corresponding to the second exon sequence of the *NRF2* gene were designed; E2/89-68 is a downstream primer and E2/64-35 is an upstream primer for nested PCR analysis. The 5′-RACE products were subcloned into pGEM-T Easy Vector (Promega) and sequenced with SP6 or T7 primers by an ABI PRISM 377 Genetic Analyzer (Applied Biosystems).

Ribonuclease protection assay. To generate the ribonuclease protection assay (RPA) probes, artificial NRF2 plasmids containing the promoter region followed by NRF2 cDNA were constructed by PCR. PCR primers were designed as shown in Fig. 1A. The promoter region was amplified with either Probe/A-F (Fig. 1A, a) and Exon 1-R1 (Fig. 1A, c) or Probe/B-F (Fig. 1A, b) and Exon 1-R1 (Fig. 1A, c) using the P1 phage harboring the *NRF2* gene locus as a template. The cDNA fragment containing exon 1 and exon 2 was amplified with Exon 1-F1 (Fig. 1A, d) and Probe/E2-R (Fig. 1A, e) using pcDNAI/hNRF2 as a template. *Bam*HI sites were added to the 5′-ends of the primers Probe/A-F and Probe/B-F, while an *Eco*RI site was added to 5′-end of the primer Probe/E2-R. The PCR products generated from the P1 phage and from the NRF2 cDNA were mixed and sub-cloned into the *Bam*HI/*Eco*RI sites of pBluescript II SK (+) (Stratagene). The hybrid hNRF2 plasmids were linearized by *Not*I digestion and used as templates for antisense RPA probes that were synthesized in the presence of [α-^{32}P]dCTP (Promega). Total RNA (30 μg) was used for hybridization with each probe, and RPA was performed in the reaction system of RPA III (Ambion). Yeast tRNA was used as a negative control. To prepare the size marker, a genomic fragment amplified with Probe/B-F and Exon 1-R2 was cloned into pGEM-T Easy Vector and the DNA sequencing reaction was performed with SP6 primer according to the Sanger method (BcaBEST Dideoxy Sequencing Kit, TaKaRa).

Human DNA isolation. DNA samples were obtained from three types of Japanese populations; 51 SLE patients, 87 COPD patients [20], and 81 healthy controls. SLE patients were diagnosed based on the criteria revised by American College of Rheumatology in 1997 [21,22]. Out of 51 SLE patients, 40 suffered from lupus nephritis as a complication and 47 were female. COPD patients were as described in a previous report [20]. Among 50 healthy controls, 25 were female and the rest were male. Genomic DNAs were isolated from whole blood using a QIAamp DNA Blood Midi Kit (Qiagen). The study protocol was approved by the Institutional Ethical Review Board of the University of Tsukuba.

Identification and genotyping of polymorphisms. Two and six sets of PCR primers were designed to amplify the promoter and the coding regions of the *NRF2* gene, respectively (Tables 1 and 2). Direct sequencing of the PCR products was performed to identify polymorphisms (ABI PRISM BigDye Primer Cycle Sequencing Ready Reaction Kit). The genotypes of SNPs were determined by directly sequencing PCR products amplified with hNrf2/P2-F and hNrf2/P2-R. Briefly, 500 ng of genomic DNA was used as a template, and PCR was performed using 200 nM of each primer, 200 nM of each deoxynucleotide triphosphate, 1× Ex *Taq* buffer, and 1 U Ex *Taq* polymerase (TaKaRa). PCR products were electrophoresed in a 2% agarose gel and purified using a QIAquick Gel Extraction kit (Qiagen). Sequence reactions were carried out using an ABI PRISM BigDye Primer Cycle Sequencing Ready Reaction Kit and genotyped by an ABI 3100 DNA Sequencer. Genotyping triplet repeat polymorphism was performed by Gene scan analysis using an ABI 310 Sequencer, determining the repetition number of the ccg triplet repeats. Cy5-modified hN/E1g-F and hN/E1g-R were used to amplify the promoter region containing the triplet repeat by PCR with 500 ng of genomic DNA, 200 nM of each primer, 400 nM of each deoxynucleotide triphosphate, 1× GC buffer II (TaKaRa), and 1.5 U Ex *Taq* polymerase (TaKaRa).

Statistical analysis of human samples. The genotypic and allelic frequencies between patients and controls were both analyzed by Fisher's exact test. The genotypic frequencies were calculated between a homozygous population of one allele and the other populations including a homozygous population of the other allele and a heterozygous population. Significance was accepted when the p value was less than 0.05.

Results and discussion

Structural analysis of the human NRF2 gene

In our initial analysis, we searched the human genome databases and found information on the *NRF2* gene structure including the location of each exon on the genome and the sequences of exon–intron boundaries

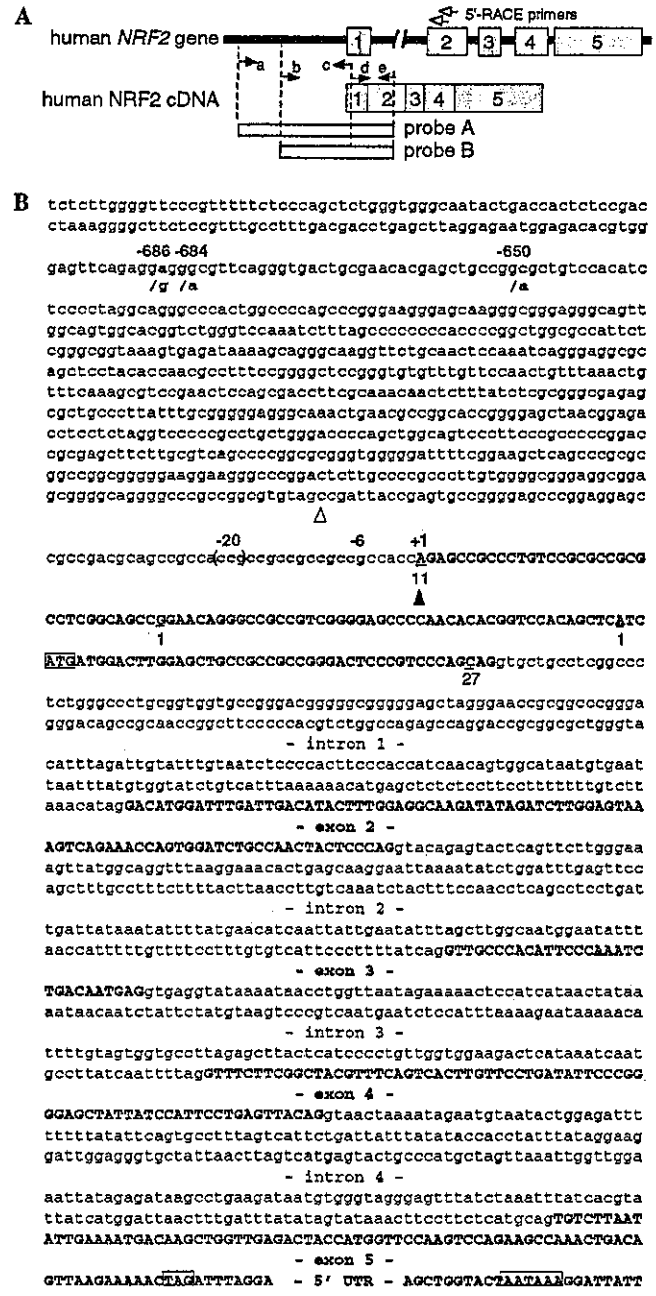

Fig. 1. Structure of the human *NRF2* gene and identification of the first exon. (A) Illustration of the human *NRF2* gene and NRF2 cDNA. Five exons were identified in the *NRF2* gene, and each is indicated by a numbered box, while NRF2 cDNA is depicted as an elongated box below. Two open arrows above exon 2 indicate the positions of the 5′-RACE primers. Five closed arrows (a–e) at the 5′ region of the *NRF2* gene and the NRF2 cDNA represent the primers for making RPA probes, which are indicated by two open bars at the bottom. (B) The sequences of the first exon and the promoter region followed by the exon-intron boundary sequences of the *NRF2* gene. The exon sequences are written in bold upper-case letters. The nucleotides at the 5′-ends of the 5′-RACE clones are underlined, and the numbers written beneath represent the obtained clone numbers. The major transcription initiation site determined by RPA is indicated by a closed arrowhead and numbered as +1, and the minor initiation site is indicated by an open arrowhead. The identified polymorphisms are highlighted in blue. The translation start codon, the stop codon, and poly(A) signal are boxed.

(Figs. 1A and B). However, we noticed that the database reports showed several different transcription start sites (BC011558, NM.006164, hCT1952818, S74017, hCT 12360, and BX649047) and, out of these six reports, four contained the same first exon harboring the translation initiation codon (BC011558, NM.006164, hCT1952818, and S74017), while the other two contained the same non-coding first exon (hCT12360 and BX649047).

In order to identify the major first exon of the *NRF2* gene, we performed 5′-RACE analysis using RNA isolated from human Jurkat cells. For this purpose, we synthesized two sequential reverse primers, E2/89-68 and E2/64-35, corresponding to the second exon sequence of the human *NRF 2* gene (Table 1 and Fig. 1A). The downstream primer (E2/89-68) was used for the first extension, while the upstream primer (E2/64-35) was used for the following nested PCR. The products of this 5′-RACE reaction were cloned, with 40 clones being analyzed further. To our surprise, all 40 clones basically shared the same exon sequence that is located approximately 30 kb upstream of the second exon. The first exon sequences of the four database reports (BC011558, NM.006164, hCT1952818, and S74017) coincided with the one identified in this analysis. The sequence of the first exon of the human *NRF2* gene shows only limited homology (70%) with that of the mouse *nrf2* gene, which is located 25 kb from the second exon.

Eleven out of 40 clones retained the longest fragment and shared the same 5′-end adenine nucleotide, while the remaining 27 clones contained shorter fragments (Fig. 1B). We tentatively assigned this 5′-end adenine as the transcription initiation site. This result indicates that a single exon was dominantly utilized for *NRF2* gene expression in Jurkat cells.

Verification of the transcription initiation site

We further asked where is the major transcription initiation site, since three different transcription start sites had been described for the first exon identified by 5′-RACE analysis (BC011558, NM.006164, hCT1952818, and S74017). The reason for these discrepancies is unclear at present, and it was important for us to verify our proposed transcription initiation site more precisely. Therefore, we performed RPA (ribonuclease protection assay) using RNA samples from Jurkat, HeLa, and Hep3B cells. The first exon and 5′-flanking sequences identified through the 5′-RACE analysis were linked to the second exon sequence to generate the RPA probes. Two probes were synthesized; probe A is 890 bp while probe B covers 556 bp (see Fig. 1A, probes A and B). RNase digestion and subsequent electrophoresis revealed several protected bands in the RNA from Hep3B cells (Fig. 2A). The most intense band was observed at 373 bp, and a minor band was observed at 443 bp. We found that both probes gave rise to protected bands of a similar size.

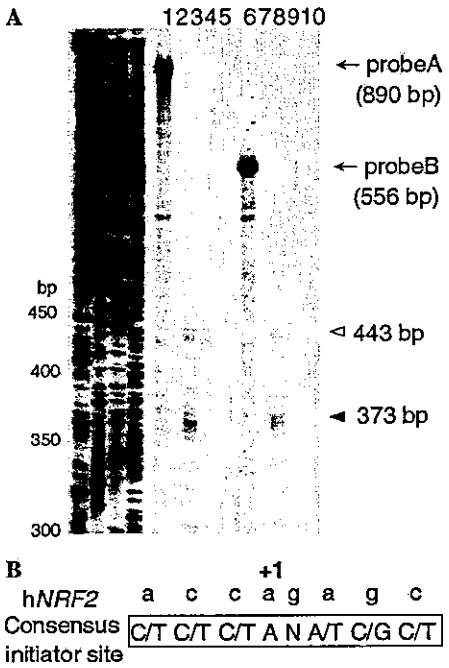

Fig. 2. Transcription initiation site of the human *NRF2* gene. (A) RPA for determining the 5′-end of the *NRF2* gene. Thirty micrograms of total RNA from HeLa (lanes 2 and 7), Hep3B (lanes 3 and 8), and Jurkat (lanes 4 and 9) cells and yeast tRNA as a control (lanes 5 and 10) was hybridized with ^{32}P-labeled probe A (lanes 2–5) or probe B (lanes 7–10), and digested with RNase A. The digested products were separated by electrophoresis with undigested probes (probe A in lane 1 and probe B in lane 6). The major and minor protected bands are indicated by closed and open arrowheads, respectively. DNA ladders applied in the four lanes on the left-hand side serve as size markers. (B) Comparison of the sequence surrounding the transcription initiation site of the *NRF2* gene and the consensus initiator site.

When we carried out the RPA experiment with RNAs derived from Jurkat and HeLa cells, the same pattern of protection was produced, but the bands were much fainter than those obtained with Hep3B cell-derived RNA. This observation implies that Nrf2 is expressed at a much lower level in Jurkat and HeLa cells than in Hep3B cells. The size of the major protected band matches that of the first nucleotide of the longest clones identified by 5′-RACE analysis (Fig. 1B). Furthermore, the nucleotide sequence surrounding the assigned transcription initiation site (Fig. 2B) corresponded well with the consensus initiator site sequence [23,24]. Overall, we conclude that the adenine nucleotide does indeed represent the transcription start site. Since the same initiation site was commonly used in three different cell lines, the single promoter is likely to specify transcription of the *NRF2* gene.

Polymorphisms identified in the promoter region of the NRF2 gene

In the hope of finding sequence polymorphisms in the coding, promoter, and upstream promoter regions of the *NRF2* gene, we sequenced approximately 1 kb of the *NRF2* promoter and regions upstream from the transcription initiation site in the P1 phage. Comparison of this sequence with the one registered in the NCBI human genome database (AC079305) revealed a single nucleotide difference. We then determined the sequences for the *NRF2* promoter and upstream regions using DNA samples from 12 healthy volunteers within the Japanese population. As a result, we found three single nucleotide polymorphisms (SNPs), including the one found in the above inspection. These SNPs were located at positions −686 (A/G), −684 (G/A), and −650 (C/A) (Fig. 3A). In addition to these SNPs, a triplet repeat polymorphism was found between −20 and −6 (four-time repetition versus five-time repetition of CCG; Fig. 3B).

We also determined the sequences for all the *NRF2* exons utilizing the 12 DNA samples from the volunteers. The primer sets used for this analysis are summarized in Table 2. However, we could not find any SNPs in the coding exons (data not shown), suggesting that the gene structure of *NRF2* is strictly conserved, and we therefore ceased our search for coding SNPs. Considering the high sensitivity of C57BL/6J strain mice to oxidative stress

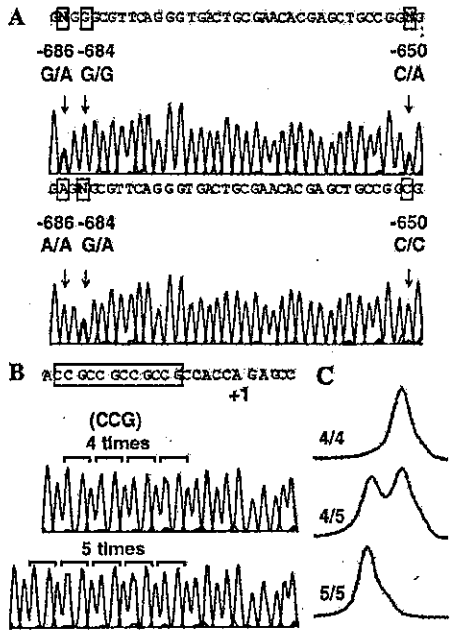

Fig. 3. Polymorphisms found in the promoter region of the human *NRF2* gene. (A) Representative electropherograms in two different patterns of the *NRF2* gene promoter region from position −685 to −649. The positions of the three SNPs, −686 G/A, −684 G/A, and −650 C/A, are indicated by arrows, and the polymorphic nucleotides are boxed in blue. (B) Representative electropherograms of homozygotes for 4- (top) or 5-time (bottom) triplet repeat polymorphisms. The transcription initiation site is numbered as +1. (C) Representative gene scan images of three different patterns of triplet repeat polymorphisms between positions −20 and −6. The homozygous pattern of 4-time repetition (top), the heterozygous pattern of 4- and 5-time repetitions (middle), and the homozygous pattern of 5-time repetition (bottom) are shown.

linked to the single nucleotide polymorphism (SNP) in the promoter region of *nrf2* gene [10], we decided to concentrate on the promoter region of the human *NRF2* gene for the search of the polymorphisms.

Study of polymorphism frequency in the Japanese population

The frequencies at which the promoter polymorphisms occurred in a healthy Japanese population were examined (Table 3, control). DNA samples were obtained from 81 healthy volunteers and genomic DNA was isolated from whole blood. SNPs were genotyped by direct sequencing (Fig. 3A), while the triplet-repeat polymorphism was determined by Gene Scan analysis (Fig. 3C). The results revealed that these polymorphisms commonly exist within the Japanese population, except for the one at position –684, for which allele A is quite rare compared to the other allele G. As for the triplet repeats, the four-time repeat is more frequent than the five-time repeat in the Japanese population.

Association of the promoter polymorphisms with human diseases

We performed a case-control study using these promoter polymorphisms in two human diseases, SLE and COPD. SLE was chosen because we previously found that female *nrf2*-deficient mice over 12 months of age often develop lupus-like autoimmune nephritis [13]. Furthermore, genome-wide linkage analysis of SLE patients pointed a genomic locus 2q31 as one of the candidate loci, which is very close to the human *NRF2* gene locus [25–27]. On the other hand, COPD was chosen as a representative of chronic inflammatory diseases. Recent analyses of *nrf2* -null mutant mice revealed that inflammation tends to be prolonged due to the reduced sensitivity of inflammatory cells to 15-deoxy-$\Delta^{12,14}$-prostaglandin J_2 (15d-PGJ_2) [28,29]. 15d-PGJ_2 was found to activate Nrf2 and regulate the late stage of inflammation, suggesting that reduction in Nrf2 activity may be one of the exacerbating causes of persistent inflammation.

We therefore collected Japanese DNA samples from 81 control subjects, 51 SLE patients, and 87 COPD patients and the four polymorphisms were genotyped (Table 3). All genotype results of the polymorphisms in the control samples were in the Hardy–Weinberg equilibrium. Because the minor allele frequency of –684G>A SNP was low (less than 7% in all groups), we excluded this polymorphism from the case control analysis. *p* values of each case-control study were calculated using genotypes and allele frequencies of three polymorphisms (Table 3). Neither genotypic nor allelic

Table 3
Genotypic and allelic frequencies of human NRF2 promoter polymorphisms in SLE and COPD patients compared with healthy controls in the Japanese population

Position	Genotype allele	Control	SLE	*p* value	COPD	*p* value
–686	G/G	27	16	0.8149[a]	29	1.0000[a]
	G/A	39	28		46	
	A/A	15	7	0.4718[a]	12	0.4047[a]
	G	93	60	0.8205	104	0.5256
	A	69	42		70	
–684	G/G	75	44		82	
	G/A	5	7	ND	5	ND
	A/A	1	0		0	
	G	155	95	ND	169	ND
	A	7	7		5	
–650	C/C	35	27	0.2754[a]	49	0.0894[a]
	C/A	41	20		31	
	A/A	5	4	0.7109[a]	7	0.6376[a]
	C	111	74	0.4862	129	0.1978
	A	51	28		45	
–20 to –6 (ccg)*n*	*n*=4/4	38	19	0.2753[a]	32	0.1832[a]
	n=4/5	34	27		43	
	n=5/5	9	5	0.8123[a]	12	0.5994[a]
	n=4	110	65	0.4847	107	0.2198
	n=5	52	37		67	

[a] Homozygous population of one allele was compared to the rest of the population including the homozygote of the other allele and the heterozygote.

frequencies were substantially different between the disease-prone and control populations (Table 3).

Concluding remarks

In order to generate a solid basis for the human genetic study of oxidative stress-related diseases, we analyzed the human *NRF2* gene structure in detail in this study. We also identified three SNPs and one triplet polymorphism within the promoter and upstream regions of the *NRF2* gene. Preliminary analyses of the link between these polymorphisms and human diseases were conducted. Although significant association was not observed in this study using a small number of patients with SLE or COPD, we still believe that Nrf2 dysfunction is one of the important prerequisites for the development of a certain group of diseases, especially those related to oxidative stress, considering the critical contribution of Nrf2 to the regulation of inflammation and elimination of ROS. Based on the connection between polymorphism of the promoter region and vulnerability to hyperoxic stress in C57BL/6J mice [10], and the absence of polymorphisms within the coding region of the human *NRF2* gene so far, we suppose that the polymorphisms of the promoter region would be indispensable tools for screening the *NRF2*-related human disorders.

Acknowledgments

We thank Drs. S. Kleeberger and T. Ohta for generous advice and Drs. Y. Kawachi, K. Hirayama, A. Hirayama, T. Ishizu, and S. Ohba for collecting human samples. We also thank Dr. X. Pan for technical help. This work is supported by grants from ERATO-JST (M.Y.), MEXT (H.M. and M.Y.), MHLW (M.Y.), and JSPS (K.Y., H.M., and M.Y.) and Special Coordination Fund for Promoting Science and Technology (H.M.).

References

[1] A. Kobayashi, T. Ohta, M. Yamamoto, Unique function of the Nrf2–Keap1 pathway in the inducible expression of antioxidant and detoxifying enzymes, Methods Enzymol. 378 (2004) 273–286.
[2] A.K. Jaiswal, Nrf2 signaling in coordinated activation of antioxidant gene expression, Free Radic. Biol. Med. 36 (2004) 1199–1207.
[3] K. Itoh, K.I. Tong, M. Yamamoto, Molecular mechanism activating nrf2–keap1 pathway in regulation of adaptive response to electrophiles, Free Radic. Biol. Med. 36 (2004) 1208–1213.
[4] K. Chan, Y.W. Kan, Nrf2 is essential for protection against acute pulmonary injury in mice, Proc. Natl. Acad. Sci. USA 96 (1999) 12731–12736.
[5] A. Enomoto, K. Itoh, E. Nagayoshi, J. Haruta, T. Kimura, T. O'Connor, T. Harada, M. Yamamoto, High sensitivity of Nrf2 knockout mice to acetaminophen hepatotoxicity associated with decreased expression of ARE-regulated drug metabolizing enzymes and antioxidant genes, Toxicol. Sci. 59 (2001) 169–177.
[6] Y. Aoki, H. Sato, N. Nishimura, S. Takahashi, K. Itoh, M. Yamamoto, Accelerated DNA adduct formation in the lung of the Nrf2 knockout mouse exposed to diesel exhaust, Toxicol. Appl. Pharmacol. 173 (2001) 154–160.
[7] M. Ramos-Gomez, M.K. Kwak, P.M. Dolan, K. Itoh, M. Yamamoto, P. Talalay, T.W. Kensler, Sensitivity to carcinogenesis is increased and chemoprotective efficacy of enzyme inducers is lost in nrf2 transcription factor-deficient mice, Proc. Natl. Acad. Sci. USA 98 (2001) 3410–3415.
[8] J.W. Fahey, X. Haristoy, P.M. Dolan, T.W. Kensler, I. Scholtus, K.K. Stephenson, P. Talalay, A. Lozniewski, Sulforaphane inhibits extracellular, intracellular, and antibiotic-resistant strains of *Helicobacter pylori* and prevents benzo[*a*]pyrene-induced stomach tumors, Proc. Natl. Acad. Sci. USA 99 (2002) 7610–7615.
[9] T. Ishii, K. Itoh, S. Takahashi, H. Sato, T. Yanagawa, Y. Katoh, S. Bannai, M. Yamamoto, Transcription factor Nrf2 coordinately regulates a group of oxidative stress-inducible genes in macrophages, J. Biol. Chem. 275 (2000) 16023–16029.
[10] H.Y. Cho, A.E. Jedlicka, S.P. Reddy, L.Y. Zhang, T.W. Kensler, S.R. Kleeberger, Linkage analysis of susceptibility to hyperoxia. Nrf2 is a candidate gene, Am. J. Respir. Cell Mol. Biol. 26 (2002) 42–51.
[11] H.Y. Cho., A.E. Jedlicka, S.P. Reddy, T.W. Kensler, M. Yamamoto, L.Y. Zhang, S.R. Kleeberger, Role of NRF2 in protection against hyperoxic lung injury in mice, Am. J. Respir. Cell Mol. Biol. 26 (2002) 175–182.
[12] A. Hirayama, K. Yoh, S. Nagase, A. Ueda, K. Itoh, N. Morito, K. Hirayama, S. Takahashi, M. Yamamoto, A. Koyama, EPR imaging of reducing activity in Nrf2 transcription factor-deficient mice, Free Radic. Biol. Med. 34 (2003) 1236–1242.
[13] K. Yoh, K. Itoh, A. Enomoto, A. Hirayama, N. Yamaguchi, M. Kobayashi, N. Morito, A. Koyama, M. Yamamoto, S. Takahashi, Nrf2-deficient female mice develop lupus-like autoimmune nephritis, Kidney Int. 60 (2001) 1343–1353.
[14] K. Itoh, N. Wakabayashi, Y. Katoh, T. Ishii, K. Igarashi, J.D. Engel, M. Yamamoto, Keap1 represses nuclear activation of antioxidant responsive elements by Nrf2 through binding to the amino-terminal Neh2 domain, Genes Dev. 13 (1999) 76–86.
[15] D. Stewart, E. Killeen, R. Naquin, S. Alam, J. Alam, Degradation of transcription factor Nrf2 via the ubiquitin–proteasome pathway and stabilization by cadmium, J. Biol. Chem. 287 (2003) 2396–2402.
[16] T. Nguyen, P.J. Sherratt, H.C. Huang, C.S. Yang, C.B. Pickett, Increased protein stability as a mechanism that enhances Nrf2-mediated transcriptional activation of the antioxidant response element. Degradation of Nrf2 by the 26 S proteasome, J. Biol. Chem. 287 (2003) 4536–4541.
[17] M. McMahon, K. Itoh, M. Yamamoto, J.D. Hayes, Keap1-dependent proteasomal degradation of transcription factor Nrf2 contributes to the negative regulation of antioxidant response element-driven gene expression, J. Biol. Chem. 278 (2003) 21592–21600.
[18] K. Itoh, N. Wakabayashi, Y. Katoh, T. Ishii, T. O'Connor, M. Yamamoto, Keap1 regulates both cytoplasmic-nuclear shuttling and degradation of Nrf2 in response to electrophiles, Genes Cells 8 (2003) 379–391.
[19] M.K. Kwak, K. Itoh, M. Yamamoto, T.W. Kensler, Enhanced expression of the transcription factor Nrf2 by cancer chemopreventive agents: role of antioxidant response element-like sequences in the nrf2 promoter, Mol. Cell. Biol. 22 (2002) 2883–2892.
[20] K. Hirano, T. Sakamoto, Y. Uchida, Y. Morishima, K. Masuyama, Y. Ishii, A. Nomura, M. Ohtsuka, K. Sekizawa, Tissue inhibitor of metalloproteinases-2 gene polymorphisms in chronic obstructive pulmonary disease, Eur. Respir. J. 18 (2001) 748–752.
[21] E.M. Tan, A.S. Cohen, J.F. Fries, A.T. Masi, D.J. McShane, N.F. Rothfield, J.G. Schaller, N. Talal, R.J. Winchester,

The 1982 revised criteria for the classification of systemic lupus erythematosus, Arthritis Rheum. 25 (1982) 1271–1277.
[22] M.C. Hochberg, Updating the American College of Rheumatology revised criteria for the classification of systemic lupus erythematosus, Arthritis Rheum. 40 (1997) 1725.
[23] O. Ferrigno, T. Virolle, Z. Djabari, J.P. Ortonne, R.J. White, D. Aberdam, Transposable B2 SINE elements can provide mobile RNA polymerase II promoters, Nat. Genet. 28 (2001) 77–81.
[24] S.T. Smale, D. Baltimore, The "initiator" as a transcription control element, Cell 57 (1989) 103–113.
[25] K.L. Moser, B.R. Neas, J.E. Salmon, H. Yu, C. Gray-McGuire, N. Asundi, G.R. Bruner, J. Fox, J. Kelly, S. Henshall, D. Bacino, M. Dietz, R. Hogue, G. Koelsch, L. Nightingale, T. Shaver, N.I. Abdou, D.A. Albert, C. Carson, M. Petri, E.L. Treadwell, J.A. James, J.B. Harley, Genome scan of human systemic lupus erythematosus: evidence for linkage on chromosome 1q in African-American pedigrees, Proc. Natl. Acad. Sci. USA 95 (1998) 14869–14874.
[26] P.M. Gaffney, W.A. Ortmann, S.A. Selby, K.B. Shark, T.C. Ockenden, K.E. Rohlf, N.L. Walgrave, W.P. Boyum, M.L. Malmgren, M.E. Miller, G.M. Kearns, R.P. Messner, R.A. King, S.S. Rich, T.W. Behrens, Genome screening in human systemic lupus erythematosus: results from a second Minnesota cohort and combined analyses of 187 sib-pair families, Am. J. Hum. Genet. 66 (2000) 547–556.
[27] J.Y. Chan, M.C. Cheung, P. Moi, K. Chan, Y.W. Kan, Chromosomal localization of the human NF-E2 family of bZIP transcription factors by fluorescence in situ hybridization, Hum. Genet. 95 (1995) 265–269.
[28] K. Itoh, M. Mochizuki, Y. Ishi, T. Ishii, T. Shibata, Y. Kawamoto, V. Kelly, K. Sekizawa, K. Uchida, M. Yamamoto, Transcription factor Nrf2 regulates inflammation by mediating the effect of 15-deoxy-$\Delta^{12,14}$-prostaglandin J_2, Mol. Cell. Biol. 24 (2004) 36–45.
[29] P. Gong, D. Stewart, B. Hu, N. Li, J. Cook, A. Nel, J. Alam, Activation of the mouse heme oxygenase-1 gene by 15-deoxy-$\Delta^{12,14}$-prostaglandin J_2 is mediated by the stress response elements and transcription factor Nrf2, Antioxid. Redox. Signal. 4 (2002) 249–257.

[CANCER RESEARCH 64, 6424–6431, September 15, 2004]

Nrf2 Is Essential for the Chemopreventive Efficacy of Oltipraz against Urinary Bladder Carcinogenesis

Katsuyuki Iida,[1,2] Ken Itoh,[2] Yoshito Kumagai,[3] Ryoichi Oyasu,[4] Kazunori Hattori,[1] Koji Kawai,[1] Toru Shimazui,[1] Hideyuki Akaza,[1] and Masayuki Yamamoto[2]

[1]Department of Urology, Institute of Clinical Medicine, [2]JST-ERATO Environmental Response Project, Center for TARA and Institute for Basic Medical Sciences, and [3]Institute of Community Medicine, University of Tsukuba, Tsukuba, Ibaraki, Japan; and [4]Department of Pathology, Northwestern University Feinberg School of Medicine, Chicago, Illinois

ABSTRACT

The induction of phase 2 detoxifying enzymes, such as UDP-glucuronosyltransferases (UGTs), in response to an array of naturally occurring and synthetic agents, such as oltipraz (4-methyl-5-[2-pyrazinyl]-1,2-dithiole-3-thione), provides an effective means of protection against a variety of carcinogens. Transcription factor Nrf2 is an essential regulator of the inducible expression of detoxifying enzyme genes by chemopreventive agents. In this study, we investigated in Nrf2-deficient mice the susceptibility to the urinary bladder-specific carcinogen *N*-nitrosobutyl(4-hydroxybutyl)amine (BBN) and the chemopreventive efficacy of oltipraz. The incidence of urinary bladder carcinoma by BBN was significantly higher in *Nrf2*$^{-/-}$ mice than in wild-type mice; invasive carcinoma was found in 24.0 and 38.5% of wild-type and *Nrf2*$^{-/-}$ mice, respectively. Oltipraz induced the phase 2 enzymes responsible for BBN detoxification in the liver and urinary bladder in an Nrf2-dependent manner. As expected, therefore, oltipraz decreased the incidence of urinary bladder carcinoma by BBN in wild-type mice but had little effect in *Nrf2*$^{-/-}$ mice. In wild-type mouse liver, oltipraz significantly induced BBN glucuronidation and decreased the urinary concentration of *N*-nitrosobutyl(3-carboxypropyl)amine, a proximate carcinogen of BBN. Importantly, BBN was found to suppress the expression of *UGT1A* specifically in the urinary bladder. This suppression was counteracted by oltipraz in wild-type mice but not in *Nrf2*$^{-/-}$ mice. These results show that Nrf2 and its downstream target genes are responsible for BBN detoxification. Furthermore, oltipraz prevents carcinogenesis by BBN by enhancing detoxification of this carcinogen in the liver and urinary bladder.

INTRODUCTION

The relationship between chemical exposure and urothelial cancer has been well established since 1895, when it was suggested that men working in the dye industry were at increased risk of bladder cancer (1). 2-Naphthylamine subsequently was determined to be one of the causative agents (2). Currently, cigarette smoking is considered a major risk factor for the development of bladder cancer in industrialized countries (1). Similarly, *N*-nitroso compounds (NOCs) have been proposed as etiologic agents of bladder cancer associated with schistosomiasis (3). NOCs also are thought to play roles in the carcinogenesis of the stomach, esophagus, and pharynx in humans (4). *N*-nitrosodibutylamine, which was first identified as a rat bladder carcinogen, has been detected as a pollutant in tobacco smoke, corrosion inhibitor, food, and rubber products (5). Although it exists in a low concentration, it is considered practically as carcinogenic to humans (6). *N*-nitrosodibutylamine is metabolized mainly in the liver, and tumor induction in the rat bladder seems to depend on the formation of two ω-oxidized metabolites, *N*-nitrosobutyl(4-hydroxybutyl)amine (BBN) and its proximate carcinogen *N*-nitrosobutyl(3-carboxypropyl)amine (BCPN; ref. 7). Oral administration of BBN to rats and mice induces cancer specifically in the urinary bladder (8). BBN-induced urinary bladder carcinogenesis in rodents is an excellent model system to understand the carcinogenic mechanisms by NOC.

Several lines of epidemiologic and experimental evidence suggest that a decreased expression in carcinogen-detoxifying enzymes, such as *N*-acetyl transferase 2 (9, 10), glutathione *S*-transferase (GST) M1 (9, 11), NAD(P)H quinone oxidoreductase (NQO1; ref. 12), and UDP-glucuronosyltransferase (UGT) 1A (13), is associated with urinary bladder cancer. The urinary bladder-specific carcinogenic effect of BBN may result, at least in part, from the metabolic fate of the compound because BCPN, the major urinary metabolite of BBN, has been shown to have carcinogenic effects on urothelial cells (14, 15). Following α-hydroxylation, BCPN and BBN are chemically cleaved to their corresponding alkylcarbonium ion that binds covalently to DNA and enhances carcinogenesis (16).

Carcinogens are normally detoxified by conjugation with water-soluble cofactors. Typical examples of such cofactors are glutathione and glucuronic acid, which are conjugated to carcinogens through the actions of GSTs and UGTs, respectively. These conjugating enzymes have been categorized as phase 2 detoxifying enzymes (17). It has been proposed that induction of phase 2 detoxifying enzyme genes plays a major role in protection against carcinogens (18). A recognized characteristic action of chemopreventive agents, including the phenolic antioxidants 2,3-butyl-4-hydroxyanisole (19) and 1,2-dithiole-3-thione (20) and the isothiocyanates (21), is their potential to induce phase 2 enzymes. Oltipraz (4-methyl-5-[2-pyrazinyl]-1,2-dithiole-3-thione) represents one of the most potent inducers of phase 2 enzymes (22, 23).

The induction of phase 2 enzyme genes is regulated by their *cis*-acting antioxidant response element (ARE) or electrophile responsive element (EpRE; refs. 24–26). Transcriptional factor Nrf2 binds to and regulates transcription through the ARE/EpRE after heterodimerizing with one of the small Maf proteins (27–29). Germline mutant mice specifically lacking the *Nrf2* gene have been established (30, 31). When we treated these mice with 2,3-butyl-4-hydroxyanisole, we found that *Nrf2*$^{-/-}$ mice lack the inducible expression of phase 2 and antioxidant enzymes, providing conclusive evidence for the notion that Nrf2 regulates their transcription (30).

An obvious hypothesis then is that *Nrf2*$^{-/-}$ mice are more susceptible to oxidative and electrophilic stresses, and this hypothesis has been tested in various contexts (32–40). For example, the forestomach tumor formation caused by benzo(*a*)pyrene is markedly increased in *Nrf2*$^{-/-}$ mice, and the chemoprotective activities of oltipraz and sulforaphane were lost (33–35). Similarly, *Nrf2*$^{-/-}$ mice are more susceptible to the acute toxicities of acetaminophen, diesel exhaust, 2,3-butyl-4-hydroxytoluene, and hyperoxia (36–40). These results argue that the Nrf2-mediated induction of phase 2 and antioxidant enzymes is critical for cellular defense against electrophilic and oxidative stresses. The results further suggest that oltipraz prevents

Received 5/30/04; revised 7/9/04; accepted 7/21/04.

Grant support: JST-ERATO, JSPS, the Ministry of Education, Science, Sports and Technology, the Ministry of Health, Labor and Welfare, the Atherosclerosis Foundation, and the Naito Foundation.

The costs of publication of this article were defrayed in part by the payment of page charges. This article must therefore be hereby marked *advertisement* in accordance with 18 U.S.C. Section 1734 solely to indicate this fact.

Requests for reprints: Masayuki Yamamoto, Center for TARA, University of Tsukuba, 1-1-1 Tennoudai, Tsukuba 305-8577, Japan. Phone: 81-298-53-6158; Fax: 81-298-53-7318; E-mail: masi@tara.tsukuba.ac.jp.

chemical carcinogenesis by inducing Nrf2-regulated cytoprotective enzymes.

The contribution of the Nrf2 regulatory pathway in protection against urinary bladder carcinogenesis requires clarification, even though a large number of studies on chemically induced cancer formation have been reported. Thus, we investigated the susceptibility of *Nrf2*$^{-/-}$ mice to the urinary bladder-specific carcinogen BBN and the preventive efficacy of oltipraz in these mice. In wild-type mice, oltipraz up-regulated the detoxification activity of carcinogens in the liver and consequently decreased the BCPN concentration in the urine. Importantly, oltipraz also induced the expression of phase 2 enzyme genes in the wild-type urinary bladder and counteracted BBN-induced suppression of *UGT1A* gene expression. In *Nrf2*$^{-/-}$ mice, loss of Nrf2 significantly enhanced susceptibility to BBN and largely abolished the chemopreventive efficacy of oltipraz. These results show that the cellular defense enzymes under the regulation of Nrf2 play key roles in preventing urinary bladder carcinogenesis.

MATERIALS AND METHODS

Reagents. BBN was purchased from Tokyo Kasei (Tokyo, Japan). The Chemoprevention Branch of the National Cancer Institute (Bethesda, MD) provided the oltipraz. UDP-glucuronic acid (UDPGA) was purchased from Sigma (St. Louis, MO). Dr. Yukio Mori (The Gifu Pharmaceutical University, Gifu, Japan) provided the BCPN.

Animals. Nrf2-deficient mice of ICR/129SV background have been established at the University of Tsukuba (Tsukuba, Ibaraki, Japan; ref. 30). A colony of ICR/129SV background mice were backcrossed for nine generations with C57BL/6 mice, which were purchased from CLEA Japan (Tokyo, Japan). Mice were housed in stainless steel cages in an animal room maintained at 24 ± 2 °C. Mice were maintained with a 12-hour light/dark cycle and fed a purified AIN-76A diet (Oriental MF; Oriental Yeast Co., Tokyo, Japan) and water *ad libitum*.

BBN-Induced Bladder Carcinogenesis. Oltipraz was fed *ad libitum* at the concentration of 250 mg/kg diet from 1 week before carcinogen administration until termination of the study 18 weeks later. BBN was dissolved in tap water to a concentration of 0.05% and supplied *ad libitum* for 8 weeks with the dark bottles. After the experimental period, mice were analyzed by autopsy. Urinary bladders were removed and inflated with and fixed in 10% buffered formalin. Each bladder then was sectioned sagittally, and each cup-shaped area was cut into four pieces. These eight strips of bladder tissue were serially embedded in one block of paraffin, cut into thin sections, and stained with H&E. Bladder lesions were histologically diagnosed according to the criteria of Oyasu *et al.* (41).

RNA Blot Analysis. Total RNAs from liver and whole urinary bladder were extracted with Isogen (Nippon Gene, Toyama, Japan) according to the manufacturer's instructions. Total RNAs (10 μg) were separated by 1.5% agarose gel electrophoresis containing 2.2 mol/L formaldehyde and transferred to nylon membrane. DNA probes for Nrf2 and UGT1A6 have been described previously (37), and Dr. Kimihiko Satoh (Hirosaki University School of Medicine, Hirosaki, Japan) provided probe for GSTπ (GSTP). DNA probes for UGT1A7 and total UGT1A were prepared by PCR using the following sets of primers: UGT1A7 sense primer, 5′-GCAGATGGTTGTGGAGAAACTC-3′; with antisense primer, 5′-GAGGTCTGTCATAGTCACTGG-3′; total UGT1A sense primer, 5′-AGCCTATGTCAACGCCTCTGG-3′; and with antisense primer, 5′-CCACTTCTCAATGGGTCTTGG-3′.

Establishment of Primary Cultures of Mouse Urothelial Cells. We adopted and modified the protocol to isolate bladder epithelium from male mice (42). Briefly, after the whole bladder was excised, it was everted to expose the mucosal surface. The bladder was digested in 20 units of dispase (Life Technologies, Inc., Rockville, MD) in PBS for 1 hour at 37°C. Following digestion, the bladder mucosa was gently detached from the underlying muscle tissue using fine-toothed forceps with coarse tips under a dissecting microscope. Mucosa was collected in PBS and further digested with 0.15% trypsin/EDTA at 37°C for 5 to 10 minutes. Trypsinized cells were mechanically dissociated by rigorous pipetting, filtered through a 100-μm nylon cloth, and centrifuged at 200 × *g* for 5 minutes. Approximately 5 to 10 × 10^5 cells were seeded in a 50-mm plastic dish containing a 1:1 mixture of serum-free keratinocyte medium and DMEM with 5% (v/v) fetal bovine serum, epidermal growth factor (5 ng/mL), bovine pituitary extract (50 μg/mL), cholera toxin (30 ng/mL), penicillin (100 units/mL), and streptomycin (1 μg/mL). The reagents used for this culture experiment were from Life Technologies.

Immunoblot Analysis. The nuclei of mouse hepatic cells and primary mouse urothelial cells prepared as described previously were solubilized with SDS-sample buffer without loading dye and 2-mercaptoethanol. Protein concentrations were estimated by BCA protein assay (Pierce, Rockford, IL). Proteins were separated by 6.0% SDS-PAGE and electrotransferred onto an Immobilon membrane (Millipore, Bedford, MA). Anti-Nrf2 antibody was used as described previously (32). Drs. Shigeru Taketani (Kyoto Institute of Technology, Kyoto, Japan) and John Hayes (University of Dundee, Dundee, United Kingdom) provided anti-heme oxygenase 1 (HO-1) and anti-GSTA1/A2 antibodies, respectively. Immunoreactive proteins were detected using horseradish peroxidase-conjugated anti-IgG antibody and enhanced chemiluminescence (Amersham Biosciences, Piscataway, NJ).

Determination of BCPN. The urinary level of BCPN was determined as reported previously (43) with modification. The urine sample (0.1 mL) was diluted to 0.5 mL with distilled water before assay. A 3.3-μL aliquot of 12 mol/L HCl was added, and the sample was extracted with 0.5 mL of ethyl acetate three times. The organic layers were collected after centrifugation for 5 minutes at 10,000 × *g* and dried using a speed vacuum concentrator with a cooling trap <30°C. The residues dissolved in ethyl acetate were spotted onto a silica gel 70 F_{254} precoated plate (Wako, Osaka, Japan) and developed with chloroform/methanol/acetic acid (18:1:1, v/v) in the dark. The bands corresponding to BBN or BCPN (Rf = 0.68 to 0.72) were scraped off and eluted from the silica with 4 mL acetone. The eluates then were concentrated by speed vacuum as before and diluted with acetonitrile to a final volume of 0.2 mL. Samples were filtered through a MINISART RC4 filter (0.2-μm pore size; Sartorius, Gottingen, Germany) and analyzed by high-performance liquid chromatography (HPLC). The urinary BCPN level was determined with a Shimazu LC9A apparatus (Shimazu, Kyoto, Japan) on a Finepak SIL C_{18} column (Jasco, Tokyo, Japan; 250 × 4.6 mm, inner diameter) at 239 nm. Separation was performed with a mobile phase consisting of a 3:7 mixture

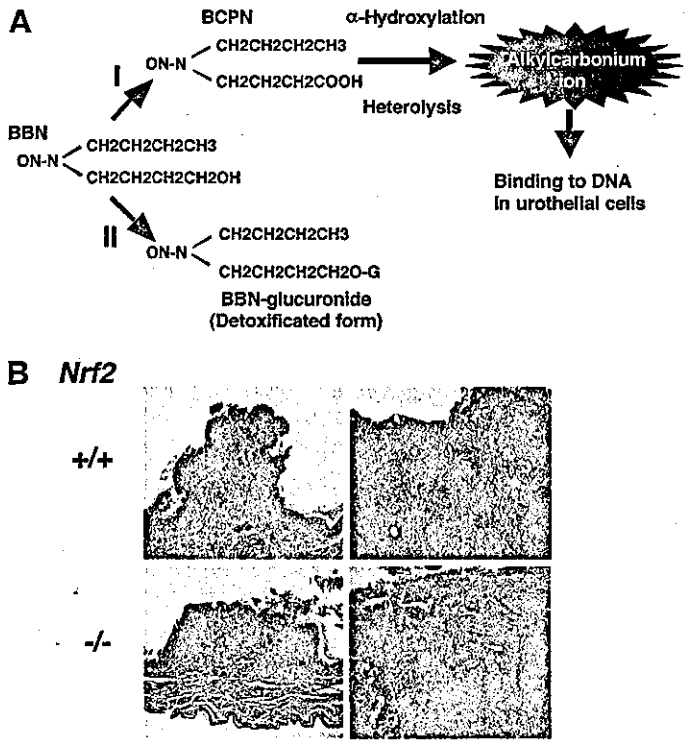

Fig. 1. BBN-induced carcinogenesis in wild-type and *Nrf2*$^{-/-}$ mouse urinary bladders. *A*, biotransformation processes of BBN; *G*, glucuronic acid. *B*, histopathologic analysis of tumor regions. Tissue sections of urinary bladder from wild-type (*top*) and *Nrf2*$^{-/-}$ (*bottom*) mice were analyzed by H&E staining. Noninvasive carcinoma (*left*) and invasive carcinoma (*right*) are shown.

Table 1 *BBN-induced carcinogenesis of the urinary bladder in wild-type and Nrf2$^{-/-}$ male mice and effect of oltipraz on the carcinogenesis*

Genotype	Oltipraz treatment	Cancer incidence Number (%)	Invasive cancer incidence Number (%)	Total number (entry number)
Wild type	−	9 (36.0)	6 (24.0)	25 (26)
	+	4 (13.8)	1 (3.4)*	29 (29)
Nrf2−/−	−	17 (65.4)*	10 (38.5)	26 (27)
	+	15 (65.2)*	6 (26.1)	22 (26)

* $P < 0.05$ compared with untreated wild-type mice.

(v/v) of acetonitrile and 20 mmol/L sodium acetate buffer (pH 4.5) at a flow rate of 1 mL/min. Under these conditions, the retention time of BCPN was 7.8 minutes. The recovery rate of BCPN from the urine was ~60% in our assay conditions.

Measurement of BBN-Glucuronide *In vitro*. Microsomes were prepared from mouse liver as described previously (44). A typical reaction mixture consisted of 100 mmol/L potassium phosphate buffer (pH 7.4), 1 mmol/L BBN, 5 mmol/L UDPGA, 0.05% Brij 58, and microsome preparation (600 μg) in a final volume of 1.0 mL. Reactions were initiated by the addition of BBN, and incubations were performed at 37°C for 30 minutes. BSA (1 mg) and 24% trichloroacetic acid (0.1 mL) were added to the incubation mixture to terminate the reaction. After centrifugation at 10,000 × *g* for 5 minutes, the supernatant (0.1 mL) was injected into the HPLC as described previously. Separation of BBN and its glucuronide was carried out with a mobile phase consisting of a 2:8 mixture (v/v) of acetonitrile and 20 mmol/L sodium acetate buffer (pH 4.5) at a flow rate of 1 mL/min.

Statistical Analyses. Data were expressed as mean ± SEM. The Student *t* test was used to determine the statistical difference among groups. The values for urinary bladder incidence were analyzed using the χ^2 or Fisher's exact probability test. A P value < 0.05 was accepted as statistically significant.

RESULTS

High Susceptibility of *Nrf2*$^{-/-}$ Mice to BBN-Induced Carcinogenesis. BBN is metabolized primarily through two pathways (45): one is alcohol/aldehyde dehydrogenase-mediated oxidation to yield BCPN, whereas the other is UGT-catalyzed conjugation to form BBN-glucuronide (Fig. 1; pathways I and II, respectively). Because glucuronide conjugation is an important process for detoxifying reactive chemicals, it has been suggested that a change in the distribution of BBN metabolites, such as a decrease in BCPN or an increase in BBN-glucuronide, might affect the incidence of tumor formation during exposure to BBN.

To elucidate the roles of Nrf2 in the prevention of urinary bladder carcinogenesis by BBN, we examined the susceptibility of *Nrf2*$^{-/-}$ mice to BBN carcinogenesis. Although *Nrf2*$^{-/-}$ mice were slightly heavier (<2.0 g) than wild-type animals, there was no significant difference in the body weight gained between the two groups during the experimental period. Several mice died before the end of the experiment (Table 1). In the group of wild-type mice, one mouse died within the experimental period, and its death was not attributable to BBN treatment. Conversely, five mice from the group of *Nrf2*$^{-/-}$ died before the end of the experiment. Autopsy revealed abdominal masses

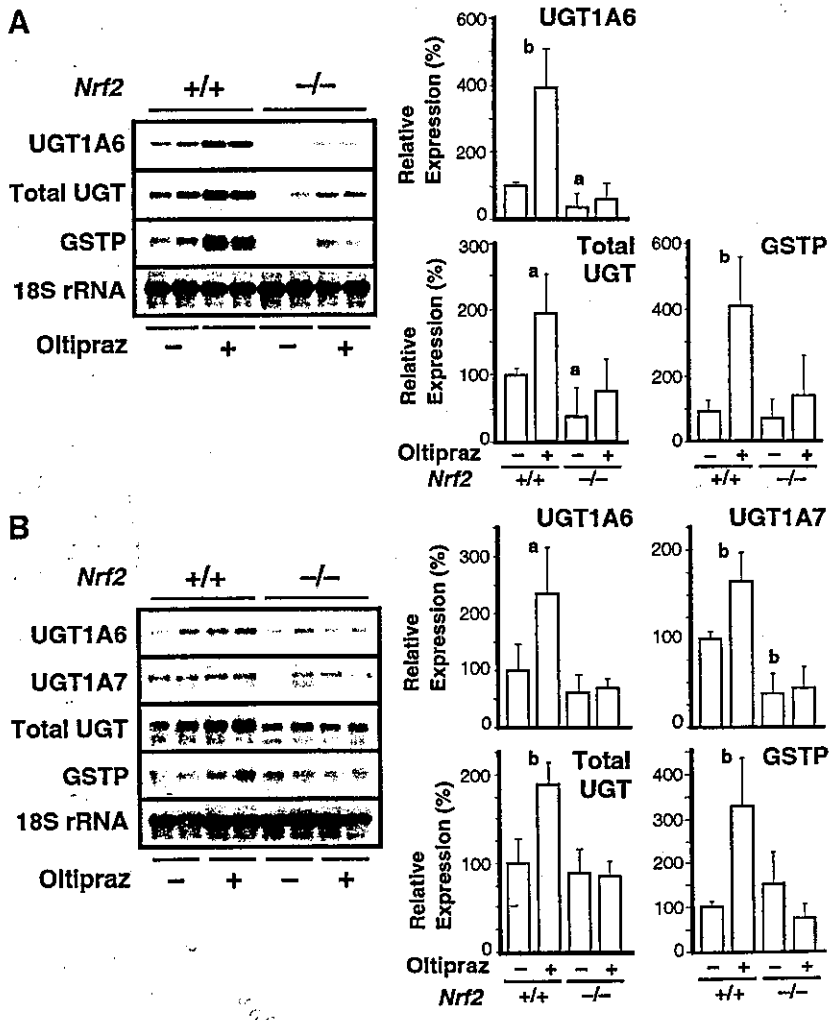

Fig. 2. Effect of oltipraz on the expression of phase 2 enzyme mRNAs in the liver and urinary bladder. *A* and *B*, effect of oltipraz on the expression of phase 2 enzyme genes in the liver (*A*) and urinary bladder (*B*) in wild-type and *Nrf2*$^{-/-}$ male mice. Oltipraz was fed at the concentration of 1 g/kg diet for 48 hours. Densitometric data of RNA blot analysis were normalized by 18S rRNA and expressed as ratios to vehicle-treated controls. Values are represented as mean ± SE ($n = 4$). *a*, $P \leq 0.05$ compared with nontreated wild-type mice. *b*, $P \leq 0.01$ compared with nontreated wild-type mice.

involving kidney and lymph nodes in three of these dead mice, apparently attributable to the BBN treatment. Bladder lesions were diagnosed histologically according to the previously described criteria (41). All of the noninvasive carcinomas were nodular rather than papillary in shape. The term "cancer" has been applied to transitional and squamous cell carcinomas because most of the lesions contained both components. No pathologic differences in noninvasive (Fig. 1*B, top* and *bottom left*) and invasive tumors (Fig. 1*B, top* and *bottom right*) were found between wild-type and *Nrf2*$^{-/-}$ mice, respectively.

Table 1 summarizes the incidence of urinary bladder cancer caused by BBN treatment. The incidence of noninvasive and invasive carcinoma was significantly higher in *Nrf2*$^{-/-}$ mice (65.4%) than in wild-type mice (36.0%; $P = 0.036$). In BBN-treated mice, invasive carcinoma was found in 38.5% and 24.0% of *Nrf2*$^{-/-}$ and wild-type mice, respectively. In wild-type mice, oltipraz treatment reduced the incidence of urinary bladder cancer by 61.6% and the incidence of invasive cancer by 85% ($P = 0.041$). However, in *Nrf2*$^{-/-}$ mice, oltipraz significantly lost its chemopreventive efficacy, although oltipraz partially reduced the incidence of invasive cancer. These results clearly indicate that detoxifying enzymes under Nrf2 regulation contribute to the cancer chemopreventive effect of oltipraz.

Expression of Phase 2 Genes in the Liver and Urinary Bladder of *Nrf2*$^{-/-}$ and Wild-Type Mice Treated with Oltipraz. To elucidate the roles that Nrf2 may play in the protection against BBN carcinogenesis afforded by oltipraz, we examined changes in the expression of detoxifying enzyme genes in the liver and urinary bladder following oltipraz treatment. For this purpose, oltipraz (1 g/kg) was added to the diet and fed to mice for 48 hours. The mRNA levels of UGT1A6, total UGT1A, and GSTP were monitored by RNA blot analysis. The constitutive expression of these detoxifying genes was 40 to 50% lower in the livers of *Nrf2*$^{-/-}$ mice than in wild-type mice (Fig. 2*A*). Although oltipraz increased the mRNA levels of UGT1A6 and GSTP by approximately fourfold and that of total UGT1A by twofold in the livers of wild-type mice, the inducible expression of these genes by oltipraz was markedly reduced in the livers of *Nrf2*$^{-/-}$ mouse (Fig. 2*A*).

Next, the expression profiles of these detoxifying enzyme genes in the urinary bladder were examined. We found that the basal level of these detoxifying enzyme mRNAs in the bladder were lower in *Nrf2*$^{-/-}$ mice than in wild-type mice (Fig. 2*B*). Oltipraz induced the expression of these enzymes in the urinary bladder of wild-type mice, but the magnitude of induction was less, approximately twofold for UGT1A6 and threefold for GSTP. The inducible expression of these genes by oltipraz was significantly abrogated in the *Nrf2*$^{-/-}$ mouse urinary bladder (Fig. 2*B*). We also examined the expression of UGT1A7 mRNA. UGT1A7 mRNA was detected in the urinary bladder (Fig. 2*B*) but not in the liver (data not shown), and the constitutive and inducible expressions were affected in the *Nrf2*$^{-/-}$ mouse urinary bladder. These results revealed that phase 2 detoxifying enzymes are expressed in the urinary bladder and that Nrf2 regulates their expression in response to electrophilic inducers.

Nrf2 Regulatory Pathway Is Activated in Liver and Urothelial Cells. We next examined Nrf2 activation by oltipraz in liver and urothelial cells. The mRNA levels of Nrf2 itself did not change substantially on treatment with oltipraz in either tissue (Fig. 3*A*). Because we carried out a targeting knockout of the *Nrf2* gene by introducing the β-galactosidase gene into the *Nrf2* locus, creating Nrf2–β-galactosidase fusion mRNA (30), we detected larger-sized mRNA in the *Nrf2*$^{-/-}$ mice. The level of the larger-sized mRNA did not change much on treatment with oltipraz (Fig. 3*A*). These observations are consistent with our contention that activation of Nrf2 correlates with nuclear accumulation of Nrf2 protein. To confirm this point further, we examined the nuclear expression of Nrf2 protein in

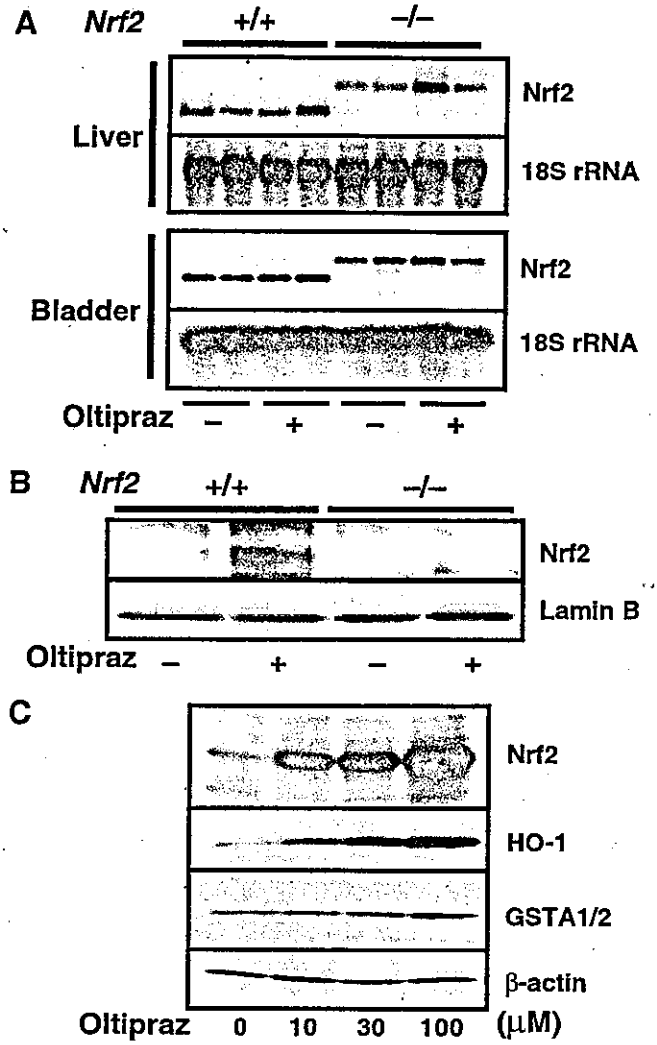

Fig. 3. Effect of oltipraz on Nrf2 activation in the liver and urinary bladder. *A*, effect of oltipraz on the expression of Nrf2 mRNA in the liver and urinary bladder of male wild-type and *Nrf2*$^{-/-}$ mice. Mice were fed oltipraz at the concentration of 1 g/kg diet for 48 hours. Densitometric analysis of RNA blot results was normalized by 18S rRNA levels and expressed as ratios to vehicle-treated controls. Values are represented as mean ± SE ($n = 4$). *B*, Nrf2 activation in mouse liver by oltipraz. Male wild-type and *Nrf2*$^{-/-}$ mice were fed oltipraz at the concentration of 1 g/kg diet for 48 hours, and hepatic nuclear extracts were examined by immunoblot analysis using anti-Nrf2 antibody. Lamin B was used as a loading control. *C*, immunoblot analyses of Nrf2, HO-1, and GSTA1/2 in mouse uroepithelial primary cell cultures. Total cell extract prepared from wild-type uroepithelial cells was treated with 10, 30, and 100 μmol/L oltipraz or vehicle for 8 hours. β-Actin was used as a loading control.

the liver after treatment with oltipraz. Immunoblot analysis showed an increased nuclear accumulation of Nrf2 protein in wild-type mice, but not in *Nrf2*$^{-/-}$ mice, following exposure to oltipraz (Fig. 3*B*).

To date, there have been no reports describing the expression of Nrf2 and its target genes in urothelial cells. However, the Nrf2-dependent expression of phase 2 enzyme genes in the urinary bladder suggests that the Nrf2 regulatory pathway is functioning in urothelial cells. We clarified that this is the case by establishing a primary urothelial cell culture system and examining the expression of Nrf2. Immunoblot analysis of total cell extracts with anti-Nrf2 antibody showed that the amount of Nrf2 protein is increased by oltipraz in a dose-dependent manner (Fig. 3*C*). Oltipraz also induced the nuclear accumulation of Nrf2 (data not shown) and the expressions of HO-1 and GSTA1/A2 (Fig. 3*C*).

Elevated BCPN Concentration in the Urine of *Nrf2*$^{-/-}$ Mice. BCPN is a proximate metabolite of BBN, and BCPN and BBN are metabolized through α-hydroxylation/spontaneous cleavage to pro-

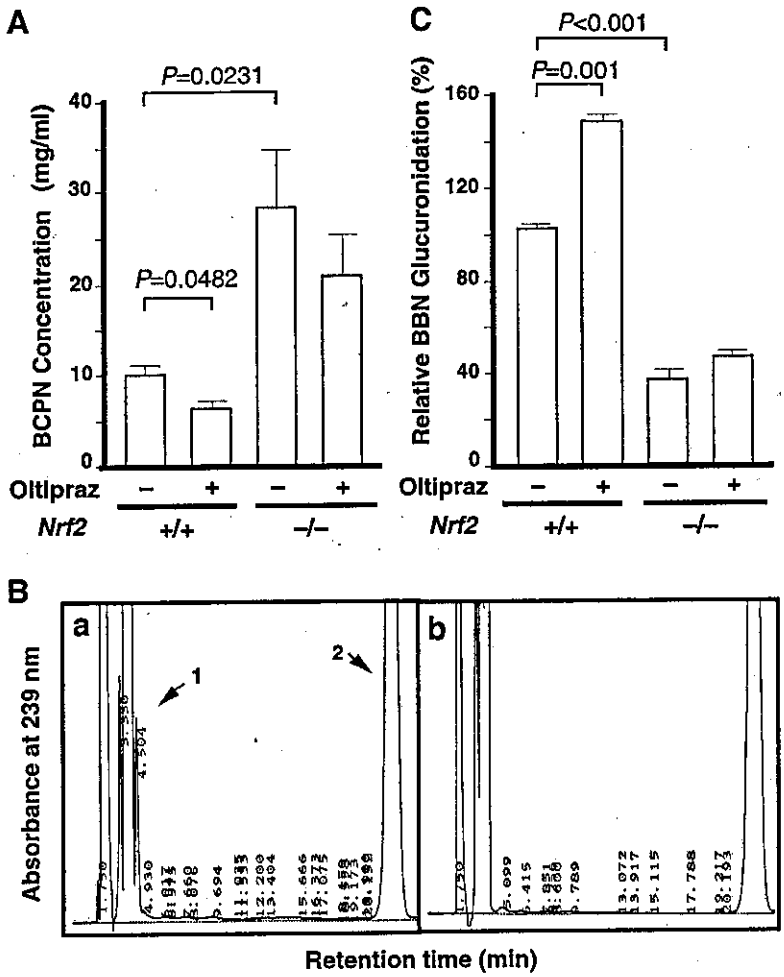

Fig. 4. Effect of *Nrf2* genotype and oltipraz treatment on the urinary concentration of BCPN after treatment with BBN and the activity of BBN glucuronidation in hepatic microsomes. *A*, Mice were fed 250 mg/kg diet of oltipraz and 0.05% BBN in drinking water for 2 weeks, and then urine samples were analyzed by HPLC. Values are represented as mean ± SE ($n = 5$). *Significantly different from nontreated wild-type mice ($P \leq 0.05$). *B*, Mice given oltipraz at the concentration of 250 mg/kg diet for 2 weeks were used. Hepatic microsomes from the animals were prepared as described in Materials and Methods. Six hundred micrograms of Brij 58-solubilized microsomes from mouse livers were incubated with 1 mmol/L BBN in the presence of 5 mmol/L UDPGA at 37°C for 30 minutes. *a*, complete system; *b*, without enzyme preparation. Peaks 1 and 2 were identified as BBN-glucuronide and BBN, respectively. *C*, The relative formation of BBN-glucuronide by liver microsomes from mice treated either with or without oltipraz treatment. Values are represented as mean ± SE ($n = 3$). *Significantly different from untreated wild-type mice ($P \leq 0.05$).

duce their alkylcarbonium ion. These reactive species can covalently bind to DNA and are associated with the formation of a butyl-guanine adduct in the urothelial DNA of animals treated with BBN (16). We hypothesized that increased carcinogenesis in $Nrf2^{-/-}$ mice is associated with a higher than normal urinary BCPN concentration. We measured by HPLC the urinary concentration of BCPN 2 weeks after administration of 0.05% BBN to mice treated either with or without oltipraz (Fig. 4*A*). Mice were fed oltipraz (250 mg/kg) 1 week before BBN administration. The urinary concentration of BCPN was significantly higher in $Nrf2^{-/-}$ mice than in wild-type mice ($P = 0.0231$). Oltipraz treatment significantly reduced the urinary concentration of BCPN in wild-type mice ($P = 0.0482$) but not in $Nrf2^{-/-}$ mice.

Oltipraz Enhanced BBN Glucuronidation Activity in Liver Microsomes. Considering that BBN glucuronidation occurs mainly in the liver, it is reasonable to assume that an increase in BBN glucuronidation in the liver would contribute, at least in part, to a decrease in BCPN concentration in the urine and consequent suppression of carcinogenesis in the urinary bladder. Therefore, we measured the glucuronidation activity of BBN in hepatic microsomes *in vitro* by HPLC. Incubation of BBN (peak 2) with the Brij 58-solubilized microsome of wild-type mouse liver in the presence of UDPGA resulted in a new product (peak 1) with a retention time of 4.5 minutes (Fig. 4*B*, *a*). This metabolite was not detected when the enzyme preparation (Fig. 4*B*, *b*), UGPGA (data not shown), or BBN (data not shown) was excluded from the incubation mixture, indicating that the product was BBN-glucuronide generated from BBN.

The basal activity of BBN glucuronidation was significantly lower in the hepatic microsomes of $Nrf2^{-/-}$ mice than in wild-type mice ($P = 0.001$). Oltipraz significantly induced the BBN glucuronidation activity in wild-type mouse liver microsomes ($P = 0.001$) but not in $Nrf2^{-/-}$ mouse liver microsomes (Fig. 4*C*). Collectively, these results suggest that the administration of oltipraz reduces the concentration of BCPN in the urine by enhancing the hepatic BBN glucuronidation activity.

BBN Decreases UGT Expression, and Oltipraz Counteracts the Suppression in Urinary Bladder. It was reported previously that *UGT1A* gene expression in cancerous human urinary bladder was either lost or decreased to a low level compared with that in normal bladder tissue (13). Such down-regulation of UGT expression in the urinary bladder may reduce the local glucuronidation activity of carcinogenic compounds, allowing their accumulation and promoting DNA mutations in the urinary bladder.

We analyzed the effect of BBN on *UGT1A* gene expression in the urinary bladder by supplementing drinking water with 0.01%, 0.05%, or 0.1% BBN for 2 weeks. The expressions of *UGT1A6*, *UGT1A7*, and total *UGT1A* were significantly decreased by BBN treatment in a dose-dependent manner (Fig. 5*A*). Importantly, this pattern of *UGT1A* suppression by BBN also was observed in $Nrf2^{-/-}$ mice (Fig. 5*B*). We tested whether oltipraz counteracts the down-regulation of *UGT1A* gene expression by BBN. Mice were given 250 mg/kg of oltipraz in the diet 1 week before carcinogen administration (0.01% BBN) in the drinking water for 2 weeks. In wild-type mice, BBN decreased the expressions of *UGT1A6*, *UGT1A7*, and total *UGT1A* by 50.1%, 54.0%, and 52.0%, respectively, whereas in $Nrf2^{-/-}$ mice, BBN markedly reduced the expressions of *UGT1A6*, *UGT1A7*, and total *UGT1A* to <10% (Fig. 5*A* and *C*). Oltipraz effectively inhibited

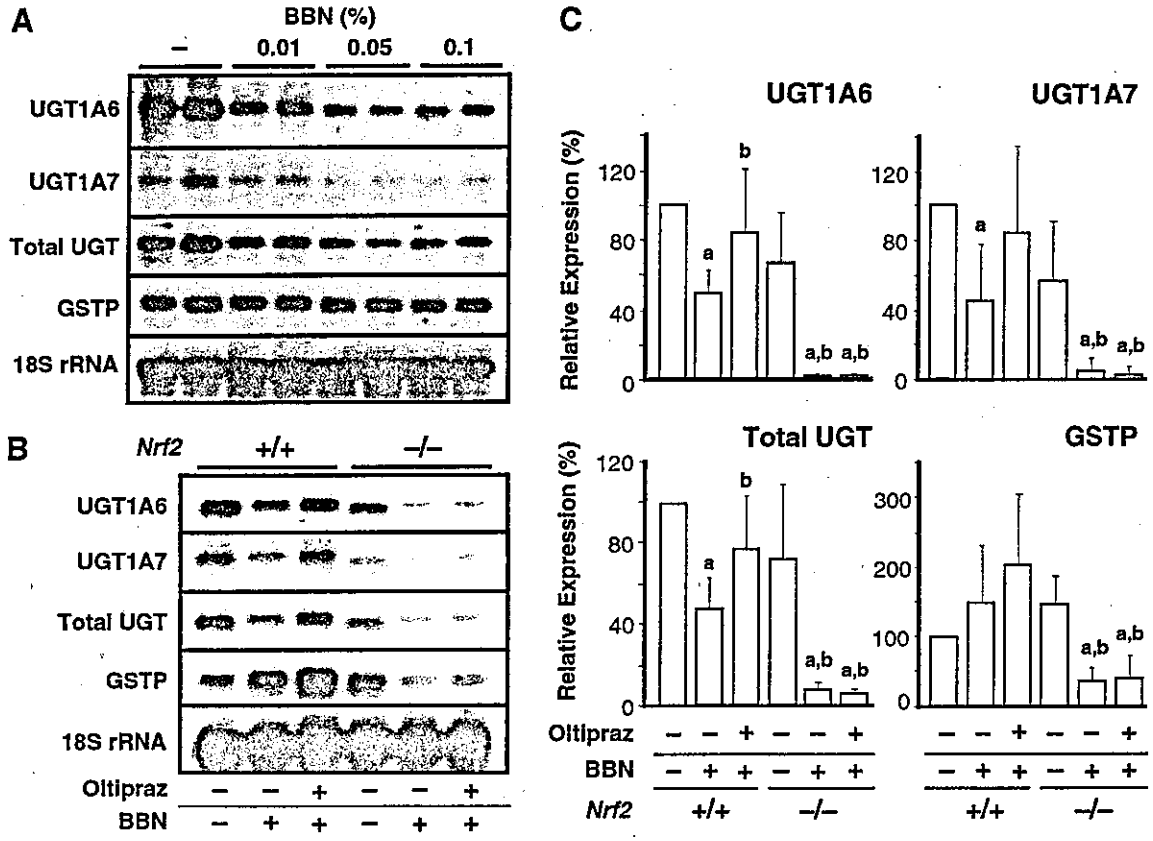

Fig. 5. Effect of BBN and oltipraz on the expressions of phase 2 genes. *A*, effect of BBN on the expressions of phase 2 genes in the urinary bladder of male wild-type mice. Mice were treated with 0.01%, 0.05%, 0.1% BBN, or vehicle in drinking water for 2 weeks. *B*, The expressions of phase 2 genes after BBN and oltipraz treatment were examined in wild-type and *Nrf2*$^{-/-}$ mice. Oltipraz was fed at the concentration of 250 mg/kg diet 1 week before carcinogen administration. BBN was given at a concentration of 0.01% in drinking water for 2 weeks. *C*, Densitometric analysis of RNA blot results was normalized by 18S rRNA levels and expressed as ratios to vehicle-treated controls. Values are represented as mean ± SE ($n = 4$). *a*, $P \leq 0.05$ compared with nontreated wild-type mice. *b*, $P \leq 0.05$ compared with BBN-treated wild-type mice.

the down-regulation of *UGT1A* genes caused by BBN in the urinary bladder of wild-type mice but completely lost its efficacy in *Nrf2*$^{-/-}$ mice (Fig. 5*B* and *C*). BBN did not suppress *GSTP* gene expression, indicating that BBN specifically targets *UGT1A* genes (Fig. 5). Thus, these results show that BBN suppresses *UGT1A* gene expression in the urinary bladder through mechanisms independent of the Nrf2 regulatory pathway.

DISCUSSION

Our study has shown that *Nrf2*$^{-/-}$ mice are more susceptible to BBN-induced carcinogenesis of the urinary bladder than wild-type mice. The elevated incidence of BBN carcinogenesis in *Nrf2*$^{-/-}$ mice was associated with the higher concentration of BCPN in the urine and lower activity of BBN-glucuronidation in the liver. Whereas oltipraz effectively reduced the incidence of urinary bladder carcinoma initiated by BBN in wild-type C57BL/6 mice, it showed little effect in *Nrf2*$^{-/-}$ mice. In wild-type mice, oltipraz significantly increased the activity of BBN-glucuronidation in the liver, an increase that correlated well with the increased *UGT1A* gene expression, and thereby reduced the urinary concentration of BCPN. Furthermore, oltipraz increased the expression of phase 2 enzyme genes and suppressed the BBN-induced down-regulation of *UGT1A* expression in urinary bladder in an Nrf2-dependent manner. Collectively, these results highlight the importance of a set of detoxifying and cytoprotective enzymes under the regulatory influence of Nrf2 in the prevention of urothelial carcinogenesis.

Epidemiologic and experimental lines of evidence also suggest that the activity of detoxifying enzymes is tightly linked to urinary bladder carcinogenesis. However, the mechanism as to how the decrease in detoxifying enzyme activity contributes to carcinogenesis of the urinary bladder remains to be clarified. It was reported previously that oltipraz, an inducer of phase 2 detoxifying enzymes, reduces the incidence of bladder cancer caused by BBN (46). Exploiting *Nrf2*$^{-/-}$ mice for the BBN-carcinogenesis experiment, this study proved that oltipraz acts to prevent the initiation of cancer through activation of detoxification enzymes under Nrf2 regulation. It is of note that oltipraz repressed the incidence of invasive cancer and urinary BCPN concentration even in *Nrf2*$^{-/-}$ mice, indicating that oltipraz exerts its chemopreventive function partially through a pathway independent of Nrf2. Oltipraz was reported to induce *GSTA2* gene expression by activating CAAT/enhancer binding protein β (47).

One salient observation in this study was that the detoxification processes in the liver and urinary bladder act simultaneously and cooperatively to prevent chemical carcinogenesis of the urinary bladder. Our current model for the roles of Nrf2 and its downstream gene products in protection against BBN carcinogenesis is summarized in Fig. 6. In this model, oltipraz prevents BBN carcinogenesis primarily through the induction of BBN glucuronidation in the liver. Oltipraz also induces phase 2 and antioxidant enzymes in the urinary bladder in an Nrf2-dependent manner. Because BBN and BCPN are metabolized to reactive species in urothelial cells, it is likely that the defense system in the urinary bladder plays a key role in the anticarcinogenic mechanism (16). Therefore, induction of Nrf2-mediated detoxifying enzymes in the peripheral urothelial cells and in liver may become an important strategy to prevent BBN-induced bladder carcinogenesis.

It has been shown that decreased expression of phase 2 detoxifying